Synthesis of Copper Oxide Nanoparticles Using Indigenous Plant Leaf Extract of Khat (*Catha edulis*) for Dye Sensitized Solar Cell Application

BY

Worku Wubet

A Thesis Submitted to Applied Chemistry Department

School of Applied Natural Science

Presented for the Partial Fulfillment of the Requirements for the Degree of

Master of Science in Chemistry (Physical Chemistry)

Office of Graduate Studies

Adama Science and Technology University (ASTU)

August, 2018

Adama, Ethiopia

Synthesis of Copper Oxide Nanoparticles Using Indigenous Plant Leaf Extract of Khat (*Catha edulis*) for Dye Sensitized Solar Cell Application

BY

Worku Wubet

Advisor: Bedasa Abdisa (PhD)

Co-Advisor: Fedlu Kedir (PhD)

A Thesis Submitted to Applied Chemistry Department

School of Applied Natural Science

Presented for the Partial Fulfillment of the Requirements for the Degree of

Master of Science in Chemistry (Physical Chemistry)

Office of Graduate Studies

Adama Science and Technology University (ASTU)

August, 2018

Adama, Ethiopia

ADVISOR'S APPROVAL SHEET

This is to certify that the thesis entitled "**Synthesis of CuO Nanoparticles Using Indigenous Plant Leaf Extract of Khat (*Catha edulis*) for Dye Sensitized Solar Cell Application"** submitted in partial fulfillment of the requirements for the degree of Master of Science in Chemistry (Physical Chemistry) has been carried out by Worku Wubet, ID № GSR/0166/09 under our supervision. Therefore, we here by recommend that the student has fulfilled the requirements and hence he can submit the thesis to the department

_____	_____	_____
Name of Advisor	Signature	Date
_____	_____	_____
Name of Co-Advisor	Signature	Date

Approval page

BY: _____ _____ _____

Student Name Signature Date

As thesis advisors, we hereby certify that we have read and evaluated this thesis paper which was done under our guidance by Worku Wubet entitled: **"Synthesis of CuO Nanoparticles Using Indigenous Plant Leaf Extract of Khat (*Catha edulis*) for Dye Sensitized Solar Cell Application "fulfills** thesis requirement for the degree of master of science in chemistry (Physical Chemistry).

1. _____ _____ _____

Advisor Signature Date

2. _____ _____ _____

Co- Advisor Signature Date

As members of the board of examiners for the M.Sc thesis open defense examination, we certify that we have read and evaluated the thesis paper prepared by Worku Wubet and examined the candidate. We recommended the thesis paper to be accepted as fulfillment for the requirements of the thesis guideline of Adama Science and Technology University/Applied Chemistry Department.

3. _____ _____ _____

Internal Examiner Signature Date

4. _____ _____ _____

External Examiner Signature Date

5. _____ _____ _____

Chair Person Signature Date

6. _____ _____ _____

Department Head Signature Date

7. _____ _____ _____

School Dean Signature Date

DECLARATION

I hereby declare that this M.Sc thesis is my original work and has not been presented for a degree in any other university, and all sources of material used for this thesis have been duly acknowledged.

Name: Worku Wubet

Signature: _____

This M.Sc Thesis has been submitted for examination with our approval as thesis advisors.

Advisor Name: Bedasa Abdisa (PhD), Signature: _____

Co-advisor Name: Fedlu Kedir (PhD), Signature: _____

Date of submission:_____

ACKNOWLEDGEMENTS

First I would like to thank almighty God who gave me strength and wisdom to complete my work successfully.

Then I would like to express my genuine heartfelt gratitude to my advisor, Dr. Bedasa Abdisa for his invaluable suggestion, comments, corrections, professional and technical guidance and friendly approach throughout my work for the successful accomplishment of this thesis.

I would like to express my deepest gratitude to my Co-adviser Dr. Fedlu Kedir, for his patience, fruitful advice and friendly approach throughout my work. Without his decisive ideas and advices this work would have not been possible.

I would like to express my thanks to the Department of Applied Chemistry, Adama Science and Technology University, for providing the necessary knowledge, assistance and facilities to conduct my research work and all administration issues which were necessary during my research work.

I would also like to thank Dr. Osman Ahemed, Department of Materials Science and Engineering, Adama Science and Technology University, who gave me great assistance and useful suggestions throughout my study. His guidance and inspiration gave me a profound influence for my work and for communicating staffs in National Twain Science and Technology University, Department of Materials Science and Engineering, Twain for SEM, EDX and UV-Vis spectroscopy data generation.

I would like to give the dearest and greatest thanks to Dr. Enyew Amare, Department of Applied chemistry, for his suggestion, support and encouragement for the area of my research work.

I would like to take the opportunity to thank Adama Science and Technology University, Department of Materials Science and Engineering for TGA-DTA and XRD data generation and Addis Ababa University, Chemistry Department for FTIR data generation and to conduct the application parts.

I acknowledge and appreciate my beloved friends all those who contributed in one way or the other to the fulfillment of this research work specially Eneyew Tilahun who is my closest friend.

My acknowledgement is also extended to Adama Science and Technology University for giving me the opportunity to join this postgraduate program and for sponsoring my study.

Finally, my cheerful thanks go to my parents and all the family members who give me moral and material support during my study.

ABSTRACT

Development of green technology is generating interest of researchers towards eco-friendly and low cost method for bio-synthesis of nanoparticles. In this study CuO nanoparticles were synthesized using copper nitrate trihydrate precursor and catha edulis extract as reducing and capping agent during the synthesis. The biosynthesized nanoparticles of copper oxide were characterized using XRD, SEM-EDX, TEM, UV-Vis and FTIR. XRD characterization confirmed that the synthesized CuO NPs possessed a well crystalline nature which perfectly matched to monoclinic structure of bulk CuO. Furthermore, the results of scanning and transmission electron microscopy and energy dispersive spectroscopy exhibited that the green synthesized copper oxide nanoparticles were spherical in shape. Optical band gap of the bio-synthesized CuO NPs was determined from UV-Vis absorbance spectra using Tauc plot and found to be 1.31, 1.39, and 1.45 eV for different proportions of precursors used. The bio-synthesized copper oxide nanoparticles were employed as electrocatalytic materials for the fabrication of counter electrode in dye sensitized solar cells (DSSCs). From the fabricated DSSCs the maximum amount of solar to electrical energy conversion efficiency was 0.165% with short circuit current density of 2.03×10^{-3} *mA/cm^2 with open circuit voltage 139 mV and fill factor of 67% this indicating that the bio-synthesized CuO NPs have a potential application for DSSCc, which is cost effective and environment friendly method for solar energy to electricity conversion.*

Keyword: *CuO, Catha edulis, Dye sensitized solar cell, green synthesis, Nanoparticles.*

TABLE OF CONTENT

Contents page

LIST OF ABBREVIATIONS

DSSCs	Dye Sensitized Solar Cells
DTA	Differential Thermal Analyzer
EDX	Energy Dispersive X-ray Spectroscopy
E_g	Band gap Energy
EMIM-I	1-Ethylene-3-Methyl Immidazolium Iodide
EMU	Electron Microscope Unit
FF	Fill Factor
FT-IR	Fourier Transform Infrared
FTO	Fluorine Doped Tin Oxide
FWHM	Full Width at Half Maximum
HOMO	Highest Occupied Molecular Orbital
IPCE	Incident Photon to Current Conversion Efficiency
ITO	Indium Doped Tin Oxide
I-V	Current – Voltage
JCPDS	Joint Committee on Powder Diffraction Standards
J_{SC}	Short Circuit Current density
LHE	Light Harvesting Efficiency
LUMO	Lowest Unoccupied Molecular Orbital
NPs	Nanoparticles
PEC	Photoelectrochemical cell
PVP	Polyvinyl Pyrolidone
QE	Quantum Efficiency
SEM	Scanning Electron Microscopy
TCO	Transparent Conducting Oxide
TEM	Transmission electron microscope
TGA	Thermal gravimetric analysis
UV –Vis	Ultra Violet Visible
V_{OC}	Open Circuit Voltage
XRD	X-Ray Diffraction

LIST OF FIGURES

LIST OF TABLES

1. INTRODUCTION

1.1. Background of the Study

The growths of global population in combination with industrial developments will pose an enormous challenge in meeting the rising energy demand in the near future. As a result the worldwide need for energy is expected to keep increasing at 5% each year (Enerdata, 2011). Fossil fuels, such as coal, oil and natural gas, provide the largest part of world electricity generation. However, the reserves of these non-renewable resources are quite limited, leading to the soaring prices of fossil fuels in recent years. Moreover, the combustion of fossil fuels produces 40 billons Tons of greenhouses gases which are exhausted to atmosphere and believed to impose a significant impact on global warming and climate change (William *et al*., 2014). The rising energy demand, coupled with environmental concerns, as well as the higher prices of fossil fuels have motivated researchers to seek alternative environmentally-friendly low-carbon energy sources.

Renewable energy sources, such as solar, hydro power, wind power, biomass, tidal and waves, geothermal heat and ocean thermal energy, have been the potential to meet the rising energy demand, and are expected to play an essential role in moving the world to a more secure, reliable and sustainable energy system (World Energy Outlook, 2018).

Solar energy is the most abundant permanent energy resource on earth and the only choice that can satisfy huge and steadily increasing demand. Unlike wind power and hydro energy, it spread out more evenly in the world and it is essentially inexhaustible because it is radiation from the sun and there is a large quantity of solar radiation accepted on the earth every day. The supply of the energy from the Sun to the Earth is 3×10^{24} joules a year, which is nearly 104 times more than the world's energy consumption per year (Won *et al*., 2015). Even if only 0.1% of this energy can be converted at an efficiency of only 10%, it would be four times the world's total generating capacity (World Energy Council, 2016). Therefore, solar energy would be a prospective substitution of fossil fuels because of its wide availability, relative low cost and a potentially more secure sustainable energy source. A solar cell is a semiconductor device that converts solar energy into electricity by photovoltaic effect.

Currently, the most commercially successful solar cells are based on inorganic silicon semiconductors, made of p-n junctions. However, the need for highly purified silicon, expensive manufacturing processes, which needs high energy consumption and releases harmful emissions to the environment that

causes pollution and also requires full sunlight for optimal performance, has restricted their worldwide use. These constraints encouraged the search for environmentally friendly and low cost solar cells. In this regard, hybrid solar cells based on organic and inorganic compounds are promising and cost effective alternatives for photovoltaic energy sectors due to very low production costs such as, cheap manufacturing processes and the high performance/price ratio. As a result, the solar cell system fabricated in this project is dye sensitized solar cell, which is a promising alternative to conventional silicon solar cell and effectively utilizes a property of nanocrystalline wide band gap semiconductor porous electrode (Hee *et al*., 2013).

The field of nanotechnology is one of the most active areas of research in modern materials science. Nanoparticles usually referred to as particles with a size approximately extending from 1 nm up to 100 nm in length in at least one dimension (Hutchison, 2008), exhibit completely new or improved properties based on specific characteristics such as size, distribution and morphology. The application of nanoscale materials and structures is an emerging area of nanoscience and nanotechnology. Nanomaterials provide solutions to technological and environmental challenges in the areas of solar energy conversion, catalysis, medicine, and water-treatment (Sangiliyandi *et al*., 2009). Nanomaterials particularly metallic nanomaterials have assumed a great deal of importance as they often display unique and considerably modified physical, chemical and biological properties as compared to their counterparts of the macro scale (Fayaz *et al*., 2011).

In recent years, much attention has been paid to metal oxide nanoparticles, which exhibit novel chemical and physical properties owing to their extremely small dimensions and high specific surface area. Specifically, these small particles are interesting materials for research on catalysts with specific activity and selectivity (Kessler, 2011). So, a burst of research activity is witnessed in recent years in the area of synthesis and fabrication of different size sand shapes of metal oxide nanoparticles. Nanometer sized particles display many interesting optical, electronic, magnetic and chemical properties yielding applications in several fields: biomedicine, diagnostic, drug delivery systems and sensor, catalysis, optics and antimicrobial activities (Katwal, 2015).

The synthesis of metallic oxide nanoparticles is an active area of academic and, more importantly application research in nanotechnology. A variety of chemical and physical procedures such as chemical reduction, electrochemical reduction, chemical vapor deposition, thermal decomposition and solvothermal reduction (Tang *et al*., 2006); have been reported for synthesis of metallicnanoparticles.

However, these methods are fraught with many problems including use of toxic solvents, generation of hazardous by-products, and high energy consumption. Accordingly, there is an essential growing need to develop clean, reliable, biocompatible, cost-effective, environmentally benign, and sustainable procedures for synthesis of metallic oxide nanoparticles that do not use toxic chemicals which encouraged more and more researchers to exploit biological systems as possible eco-friendly nano-factories. A promising approach to achieve high yield, low cost, environment-friendly and sustainable procedures for the synthesis of metal oxide nanoparticles is to exploit the array of biological resources in nature. Indeed, over the past several years, plants, algae, fungi, bacteria, and viruses have been used for production of low cost, energy-efficient, and nontoxic metallic nanoparticles (Taleb *et al*., 1998).

Biological systems using microorganisms such as algae, fungi, bacteria, enzymes, mushrooms and plant leaf extracts have been suggested as possible eco-friendly alternatives to chemical and physical methods for the synthesis of low-cost, energy efficient, and non-toxic metallic nanoparticles. Use of plant extracts for synthesis of nanoparticles could be advantageous over other environmentally benign biological processes as this eliminates the elaborate process of maintaining cell culture (Taleb *et al*., 1998) and the advantage of using plants for the synthesis of nanoparticles is that they are easily available, safe to handle and possess a broad variability of metabolites that may aid in reduction.

Biosynthesis of metal oxide nanoparticles by plant extracts is currently under exploitation. The uses of *Azadirachtaindica* (Neem) (Shankar *et al*., 2004), *Emblicaofficinalis* (amla, Indian Gooseberry) (Amkamwar *et al*., 2005), mangosteen leaf, *Chenopodium album* (Veerasamy *et al*., 2011) and many others have been reported. Studies have indicated that biomolecules like proteins, phenols, and flavonoids not only play a role in reducing the ions to the nanosize, but also play an important role in the capping of the nanoparticles (Vedpriya, 2010).

Therefore, in this study Copper oxide (CuO) nanoparticle was synthesized using leaf extracts of Khat (*Catha edulis*) and used as cathode/counter electrode for the application of dye sensitized solar cell.

1.2. Statement of the Problem

In recent years the most common methods to obtain energy are based on fossil fuels and many other non renewable sources. But these common methods to obtained energy are associated with high level of CO_2 emissions (Realpe *et al.*, 2015). As a result of these CO_2 emissions in to the natural environment which causes global warming, it is necessary to develop alternative methods to generate green energy (Dye

sensitized solar cell) using green synthesized nanoparticles. During the last decades different researches were done on DSSCs using platinum sputtered conducting glass usually serves as the counter electrode in a typical DSSC. It is known that platinum is extremely expensive and its reserve is quite limited. Meanwhile, the fabrication of Pt counter electrode needs heat treatment and it is unfavorable for the development of flexible plastic substrate. So there is an urgent need to explore alternative Pt-free materials with a cheaper price as the counter electrode in the large scale production of DSSCs. In fact, quite a few alternative materials, such as carbon materials and conducting polymers have been used and investigated to replace Pt. In recent years, transition metal oxides, such as CuO is used for the application in DSSCs as counter electrodes (Jitendra *et al*., 2015). The maximum conversion efficiency obtained in using CuO nanoparticles (NPs) as counter electrode was nearly the same as that of the reference cell with Pt counter electrode (Wu *et al*., 2008). To the knowledge of the researcher, there has been no research work on the synthesis of CuO nanoparticle using Khat (*Catha edulis*) leaf extract as a reducing agent for the application of dye sensitized solar cells (DSSCs).Therefore, this research project was planned to synthesize CuO NPs using indigenous plant leaf extract of *Catha edulis* for DSSCs application.

1.3. Objectives of the Study

1.3.1. General Objective

The general objective of this study is to synthesize CuO nanoparticles using indigenous plant leaf extract of Khat (*Catha edulis*) for the application of dye sensitized solar cells.

1.3.2. Specific Objectives

The specific objectives of this study are:

- To synthesize CuO nanoparticles using leaf extracts of *Catha edulis*
- To characterize the synthesized CuO nanoparticles using TGA-DTA, XRD, SEM-EDX,TEM, UV-Vis and FTIR techniques
- To extract natural pigment from the roots of *kniphofia schemperi* for photo-sensitization in DSSCs.
- To fabricate DSSCs using CuO nanoparticles as a counter electrode
- To characterize DSSCs using J-V and IPCE techniques

1.4. Significance of the Study

This study provides information on green synthesis of CuO NPs using plant extract of *Catha edulis* (Khat) as a safer alternative method than conventional synthesis method. Furthermore, this work also explores the potential application of biologically synthesized CuO NPs as a counter electrode in DSSCs to replace Pt – sputtered counter electrode which is expensive. Moreover, the work also opens an opportunity and could be taken as one of the basis for interested researchers to work on this area.

1.5. Scope of the Study

This research work was limited to synthesis of CuO NPs using Khat extract for DSSC counter electrode application.

2. LITERATURE REVIEW

Nanoscience involves the study of materials on the nanoscale level between approximately 1-100 nm in length in at least one dimension (Hutchison, 2008) and the study of how to control the formation of two- and three-dimensional assemblies of molecular scale building blocks into well-defined nanostructures or nanomaterials (Rosi and Mirkin, 2005). Nanotechnology is the application of science and technology to control matter at the molecular level, which is also referred to as the ability for designing, production, characterization and application to structures, devices and systems by controlling shape and size at the nanometer scale. Nanotechnology emerges from the physical, chemical, biological and engineering sciences where novel techniques are being developed to probe and manipulate single atoms and molecules. The technology springs from advancements in material science the ability to fabricate nanoscale materials in a uniform and reliable manner, at reasonable scale and cost and has turned many of our dreams true by enabling construction of micro/nanodevices (Uskokovic, 2008).

Nanomaterials have broad applications in a variety of fields because of their unusual and size dependent optical, magnetic, electronic and chemical properties (Burda *et al*., 2005). Nanoparticles are characterized by an extremely large surface area to volume ratio and their properties are determined mainly by the behavior of their surface (Hodes, 2007). The applications of nanoparticles are well known in the fields of cosmetics and pharmaceutical products, coatings, electronics, polishing, semiconductors and catalysis. The design and preparation of novel nanomaterials with tunable physical and chemical properties remains a growing area. Nanobiotechnology is an emerging area of opportunity that seeks to fuse nano/micro fabrication and biosystem to the benefit of both. Increasing awareness towards green chemistry and other biological processes has led to the development of simple and ecofriendly approaches towards the synthesis of nanomaterials (Hsiao *et al*., 2006).

2.1. CuO Nanoparticles

Cupric oxide or CuO is also called black copper or Copper (II) oxide or tenorite and is named after Prof. Michela Tenore, an Italian botanist at the University of Naples, Italy. It is a secondary copper mineral, a rare earth metal, and the most stable form of oxidized copper and is found in the oxidized zone of hydrothermal copper deposits, a volcanic sublimate. Cupric oxide belongs to the monoclinic crystal system, with a crystallographic point group of 2/m or C2h. The space group of its unit cell is C2/c (Li *et al*., 2005).

The native Cu vacancies in CuO makes it a p-type semiconductor and the band gap value is 1.2 -1.9 eV (Song *et al*., 2004). Each atom in CuO has four nearest neighbors. In (110) plane each Cu atom is linked to four nearly co-planar oxygen atoms at the corner of the parallelogram. The oxygen atom is coordinated to four Cu atoms in the form of a distorted tetrahedron. Figure 1a and b shows the color and crystal structure of copper oxide nanoparticle respectively.

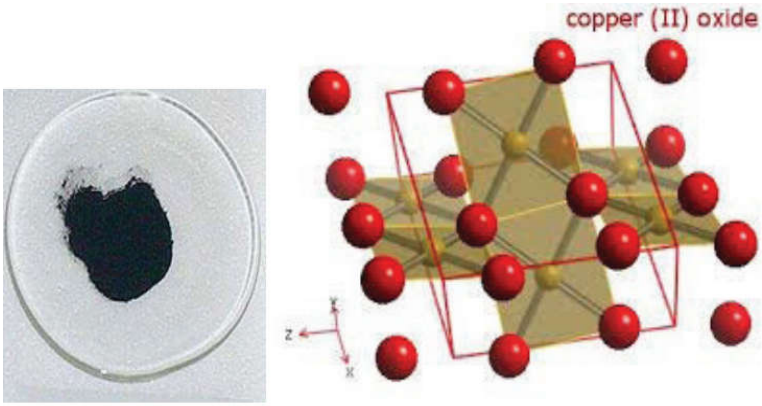

Figure 1. (a) Color of CuO (b) Crystal Structure of CuO

2.2. Synthesis of CuO Nanoparticles

Nanoparticles can be formed by two approaches: top-down (comminution and dispersion) or bottom-up (nucleation and growth) (Rahman *et al*., 2009). Top-down approach is making use of the starting bulk materials of the same materials that going to be synthesized and applying energy to break down the large materials into smaller fragments. Sources of energy can be mechanical, thermal or chemical. However, there is a disadvantage associated with this method whereby this will be creating particles with wide size distribution. To overcome this, bottom-up method was introduced as it is considered simpler and more favorable in synthesizing nanoparticles in size less than 100 nm whereby it was like building the atoms one by one, first started with a simple metal salt, slowly converts it from ions to elemental atoms by chemically eventually clumped and grown in the form of nanosize particles (Rahman *et al*., 2009). Generally, the methods for the synthesis of nanoparticles are usually classified into three categories: the physical, chemical and biological techniques (Ghorbani, 2014).

2.2.1. Physical Method

The physical method consists in the reduction of bulk solids to smaller portions in very fine grains through a grinding process, either by using acidic substances or by the application of energy sources. The grinding process is the most representative example of the physical methods, where highly efficient mills are used to separate the nanomateric sized particles. However it has not been a reliable system to obtain metallic nanoparticles because, generally, the obtained particles are larger than 100 nm, which could not be considered as nanometric size. Another disadvantage of this technique is that the applied energy for grinding must be continuous and it can infer energetic changes into solids producing a significant imbalance, which lead to a decrease of values in the energy activation. In fact, probably it is one of the oldest methods but it is not currently used to obtain CuO NPs with regular size and defined morphology. In general the physical method involves the use of costy equipment, high temperature, pressure and large surface area is required for setting up of machines and during the process it involves the use of costy chemicals (Khodashenas and Ghorbani, 2014).

Wasan *et al* reported Preparation and Characterization of CuO nanoparticles by Laser Ablation in NaOH Aqueous Solution (Wasan *et al*., 2014).

Muniz *et al* reported Characterization of Copper oxide nanoparticles obtained by laser ablation in liquids (Muniz *et al.,* 2014).

2.2.2. Chemical Method

Nanoparticles can be synthesized by various chemical methods such as sol-gel method, precipitation, hydrothermal synthesis, chemical reduction, thermal decomposition, electrochemical method and wet chemical method (Joshua *et al*., 2014). Conventional chemical methods for nanoparticles synthesis are associated with various disadvantages such as expensive, involve the use of chemicals, time consuming and pose environmental threats by generating toxic solvent and waste products which leads to a growing need to develop greener, environmentally friendly approach in synthesizing the metal nanoparticles. It has been reported that many of the biological systems such as bacteria, fungi, algae, plants and human cells can be used to convert metal ions into metal nanoparticles (Makarov *et al*., 2014).

Chemical synthesis is currently the most used and functional method, which involves condensation of atoms or molecular entities from the gaseous phase or from a solution to obtain nanoparticles with specific size and morphology; these properties are adjusted with the synthesis parameters such as temperature, precursor concentration, stabilizer agent, or solvent (Ghorbani, 2014). This method for the

CuO NPs synthesis shows the relation ratio between the precursor, the reducing agent, stabilizing agent, and the solvent. Among the chemical methods, the chemical reduction of copper salts is easy and simple to obtain CuO NPs with controlled size and morphology (Kotov, 2003).

Thi Tran and Viet Nguyen reported copper oxide nanomaterials prepared by solution methods, some properties, and potential applications (Thi and Viet, 2014).

Jyoti *et al* reported synthesis of copper oxide nanoparticles using simple chemical route (Jyoti *et al.,*2014).

Ismat *et al* reported preparation and characterization of copper oxide nanoparticles synthesized via chemical precipitation method (Ismat *et al.,* 2015).

The chemical reaction is sensitive to the aqueous media and air conditions, where the surface of the nanoparticles is highly oxidizing, so that sometimes it is necessary to use inert environmental conditions (nitrogen or argon atmosphere) or surface-active substances to protect the nanoparticles surface, like ligand agent, surfactants, soluble polymers, weak acids, and so forth The chemical method of synthesizing NPs involves the use of toxic chemicals which can prove to be hazardous for the environment and the person handling it. One way to overcome this drawback is synthesis of nanoparticles by green synthesis methods in general and using green plants in particular which is environmentally friendly and cost effective (Song *et al*., 2004).

2.2.3. Green Synthesis (Biosynthesis) Method

According to the 12 principles of green chemistry, synthesis of nanoparticles by using plant extract and microorganism has an advantage over conventional methods (Amkamwar *et al*., 2005). This approach provides a safer alternative to produce nanoparticles with desired physical and chemical properties. However, there are certain limitations to be taken note of during synthesis part as different synthesis methods could give different types of nanoparticles. Firstly, the size and shape of nanoparticles formed depends on the types of green synthesizer used, different amount of extract used, experiment parameters and these factors could lead to subsequent changes in nucleation process and number of functional groups deposited on the existing nanoparticles surface to avoid agglomeration. Due to the wide applications in diverse branches of advanced scientific fields, more and more researchers have been focused on the synthesis of CuO NPs in different routes (Devi and Singh, 2014).

The need for biosynthesis of nanoparticles rose as the physical and chemical processes were costly and often physical and chemical synthesis methods lead to the presence of some toxic chemical species adsorbed on the surface that may have adverse effects in medical applications (Subhan *et al*., 2014). So in the search for cheaper pathways for nanoparticle synthesis, scientists used microorganisms and then plant extracts for synthesis. Nature has devised various processes for the synthesis of nano and micro- length scaled inorganic materials which have contributed to the development of relatively new and largely unexplored area of research based on the biosynthesis of nanomaterials (Parashar *et al*., 2009).

Due to the wide applications in diverse branches of advanced scientific fields, more and more researchers have been focused on the synthesis of CuO NPs indifferent routes. Phytonanotechnology has become an upcoming new area of research for biological synthesizing method of metal nanoparticles. Plant extract is far more advantageous with the present of functional components in plants which can be used as a reducing agent and capping agent as well. This is a better method as they give excellent manipulation on controlling the particle size growth thus provide considerably stabilization during synthesizing process (Baker *et al*., 2013). By making use of plant extract, specific nanoparticles with desired size and shape can be designed for wide variety of nanotechnological applications. Various parts of the plants can be used for synthesis of metal nanoparticles including leaves, stems, roots and seeds. It has been reported that the phytochemical of primary and secondary metabolites are well known as natural resources that responsible for metal salt reduction (Sen *et al*., 2015).The degree of accumulation of metal nanoparticles is influenced by the reducing power of the plant extract with the reacting metal ions oxidation state.

Naika *et al* reported the synthesis of copper oxide nanoparticles by using *Gloriosa superba* L. for photocatalytic activity (Naika *et al*., 2015).

Another research by (Jayalakshmi and Yogamoorthi, 2014) used flowers of *Cassia alata* to synthesis CuO NPs, *Cassia alata* L. is belong to family Fabaceae which reported to have phytochemical activity. *Cassia alata* has been analyzed to contain active anthraquinones such as rhein, emodin, physcion and flavonoid a photocatalytic activity (Yunfang*et al*., 2013).

Nanoparticles exhibit many unique properties, for which they are intensely being studied in a number of research fields. Although a very little work has been done on the bio reduction of copper oxide nanoparticles but still they show a promising result. An easy and rapid synthesis of

copper oxide nanoparticles capped with peptides present in the latex of plant *Euphorbianivulia* (*Euphorbiaceae*), *Ixora Coccinea* L, *Acalyphaindica, Phyllanthus Amarus* L,*T. arjuna* bark extract(Yunfang*et al*., 2013),*Calotropis gigantean* L. for dye sensitized solar cell activity (Wu *et al*., 2008),*Malva sylvestris* L, aqueous extract of flowers of *Ocimum Sanctum*, *Carica papaya L*, *Tabernaemontana divaricate* L, *Aloe barbadensis*, *Tinospora cordifolia* etc that acts as both reducing and capping agent has been reported(Mohanpuria *et al*., 2008).

2.3. The Chemistry of Khat (*Catha edulis)*

Catha edulis, commonly known as khat, qat, chat or miraa, (Elhassan *et al*., 2014) is a shrub or small to medium sized evergreen tree that belongs to the Celastraceae family. It is cultivated as a bush or small tree, mainly in Yemen and East African Countries. Some oral traditions claim that khat originated from Yemen, however the literature indicates that khat originated from Ethiopia, specifically in Hararghe with a gradual expansion to different parts of Ethiopia, Yemen (Berhanu M. *et al*., 2014) and other parts of the world such as Somalia, Sudan, South Africa and Madagascar, Afghanistan and Turkestan.

Khat chewing has major effect on the gastro-intestinal system, central nervous system, cardiovascular system and urinary system. Central nervous system effects of khat chewing are alertness, dependence, tolerance, anxiety, depression, delusion and insomnia. Gastro-intestinal system effects of khat chewing are dental problem, stomach ulcer, constipation, oral and esophageal cancer. On cardiovascular system habitual use of khat causes hypertension, arrhythmia, myocardial infarction, stroke and death (Berhanu M. *et al*., 2014).

Khat contains a lot of chemical components that may have different effect on the body system. Many of them are alkaloids, terpenoids, flavonoids, sterols, glycosides, tannins, amino acids, vitamins and minerals. The major active ingredients in khat leaf were identified as the phenylalkylamine (-)-alpha aminopropiophenonenamed as cathinone (psycho stimulant component of khat) (Lamina, 2010) and cathine (nor-pseudo-ephedrine).

Due to its good chemical constituent this research planed to study the impact of khat leave for the synthesis of copper oxide nanoparticles as a reducing agent and capping agent.

2.4. Properties of CuO Nanoparticles

The properties of the CuO NPs depend on the synthesis method selected and they are very important for their applications in various areas, such as biomedical research, which is the most predominant. The most important feature is the size of the nanoparticles (which may be controlled during the synthesis) because it allows the tailored modeling of their optical, catalytic, electrical, and biological properties (Valodkar *et al*., 2011). These properties make them useful for multiple applications such as the development of cosmetics, pharmacological alternatives, paints, coatings, etc. (Katwal *et al*., 2015). Therefore, the applied synthesis method, the modulation of the reaction parameters and the composition of bulk material represent key aspects in the direct control of size and direct or indirect control of other important physical, chemical and biological properties.

2.4.1. Electrical Properties

Ruiz *et al* reported that the synthesis temperature might control the electrical conductivity of CuO NPs. When temperature increases from 300 ℃ to 700 ℃ during the synthesis, the electrical conductivity of the CuO NPs increases from 10^{-6} $(\Omega\ cm)^{-1}$ to 10^{-5} $(\Omega\ cm)^{-1}$ (Ruiz *et al.,* 2015).

Other researchers performed an assessment in order to investigate the electrical conductivity of CuO NPs. They used an aqueous solution of CuO NPs at different concentrations (0.12 g/L, 0.14 g/L, 0.16 g/L and 0.18 g/L), various temperatures of nanofluids, different particle sizes (89 nm, 95 nm, 100 nm and 112 nm) and concentrations of nanofluids obtained at the following temperatures: 25 ℃, 35 ℃, 45 ℃ and 50 ℃. The authors revealed that electrical conductivity grew with the increase of temperature and nanoparticle concentration. It was also noted that the electrical conductivity increased until the dimensions of the nanoparticles reached 95 nm in diameter. This study demonstrated that there is a correlation between the values of electrical conductivity and nanoparticle size (Ito *et al*., 2008).

2.4.2. Optical Properties

Compared with other properties such as electrical conductivity and field emission, optical property of CuO nanostructures has been much less investigated and discussed so far. As a p type semiconductor, a narrow band gap of around 1.2 eV was reported for bulk CuO. In fact, reported values of band gap for CuO were not in good agreement; for example, band gap in the range of 1.56 and 1.85 eV was reported for CuO thin films. In addition, the variation of band gap could also relate to quantum size effect in different CuO nanostructures (Cho, 2013).The optical properties of CuO NPs are significantly

influenced by the temperature, size and morphology (Hu *et al*., 2008). Bondarenko and Juganson reported an analysis of the transmission spectra of CuO NPs: at 400 ^{o}C, the UV-Vis spectra of synthesized CuO nanomaterial is maximum absorption was 350 nm and at 1000 ^{o}C, 367 nm, corresponding to band gap energy of 3.04 eV and 3.01 eV, respectively this higher band gap energy comes may be due to the experimental evidence of band-gap shrinkage or broadening due to the presence of impurities in semiconductors. By adding the impurities one can control the band-gap shrinkage or broadening. (Bondarenko and Juganson, 2013). Mishina *et al*. also synthesized CuO NPs by using the alcohol-thermal method and it was observed by UV-Vis that the absorption bandwidth of bulk CuO (1.85 eV) is narrower than the bandwidth of the CuO NPs (2.36 eV) (Mishina *et al*., 2011).

2.4.3. Chemical Properties

It is produced on a large scale by pyrometallurgy used to extract copper from ores. The ores are treated with an aqueous mixture of ammonium carbonate, ammonia, and oxygen to give copper (I) and copper (II) ammine complexes, which are extracted from the solids. These complexes are decomposed with steam to give CuO. It can be formed by heating copper in air at around 300-800°C (Koffyberg and Benko, 2013).

$$2\ Cu + O_2 \rightarrow 2\ CuO$$

For laboratory uses, pure copper (II) oxide is better prepared by heating copper (II) nitrate, copper (II) hydroxide or copper (II) carbonate:

$$2\ Cu\ (NO_3)_2 \rightarrow 2\ CuO + 4\ NO_2 + O_2$$
$$Cu\ (OH)_2\ (s) \rightarrow CuO\ (s) + H_2O\ (l)$$
$$CuCO_3 \rightarrow CuO + CO_2$$

Copper (II) oxide is an amphoteric oxide, so it dissolves in mineral acids such as hydrochloric acid, sulfuric acid or nitric acid to give the corresponding copper (II) salts:

$$CuO + 2\ HNO_3 \rightarrow Cu\ (NO_3)_2 + H_2O$$
$$CuO + 2\ HCl \rightarrow CuCl_2 + H_2O$$

$$CuO + H_2SO_4 \rightarrow CuSO_4 + H_2O$$

It reacts with concentrated alkali to form the corresponding cuprate salts:

$$2\ MOH + CuO + H_2O \rightarrow M_2\ [Cu\ (OH)_4]$$

It can also be reduced to copper metal using hydrogen, carbon monoxide, or carbon:

$$CuO + H_2 \rightarrow Cu + H_2O$$
$$CuO + CO \rightarrow Cu + CO_2$$
$$2CuO + C \rightarrow 2Cu + CO_2$$

2.4.4. Magnetic Properties

The magnetic properties of CuO NPs are also influenced by their dimensions (Cho, 2013). Moreover, the magnetic properties of CuO NPs strictly depend on their morphology. In a study focused on the properties of nanoparticles, CuO NPs with dimensions from 13 nm to 33 nm were obtained and showed a weak ferromagnetic interaction (Hu *et al*., 2008). On the contrary, Rao *et al*. reported that in the case of CuO NPs with dimensions between 9 and 16 nm, the peak present in zero field cooled magnetization is absent (Rao *et al*., 2009). Also, there was a bifurcation between the zero fields cooled and field cooled systems and it was observed that the system shows hysteresis at room temperature. These authors reported that the associated peak in magnetic viscosity and the relaxation of magnetization are similar to other nanoparticle systems. These studies indicate that the magnetic properties of CuO NPs may be influenced by the particle size, but are definitely also controlled by other aspects, possibly by their synthesis method, composition and ratio of bulk material and other physicochemical properties (Borgohain *et al*., 2002).

2.5. Applications of CuO Nanoparticles

CuO has been studied for its use in photoelectrochemical cells (PEC) and as a cathode in dye sensitized solar cells. CuO has a wide usage in making fibers, ceramics, and gas analyses and for welding fluxes. Cupric oxide is used as a pigment in ceramics to produce blue, red, and green and sometimes gray, pink, or black glazes. It is also used to produce cuprammonium hydroxide solutions, and used to make rayon. It is also occasionally used as a dietary supplement in animals, against copper deficiency. Copper (II)

oxide has application as a p-type semiconductor, because it has a narrow band gap of 1.2 eV. It is an abrasive used to polish optical equipment. Cupric oxide can be used to produce dry cell batteries. It has also been used in wet cell batteries as cathode, with lithium as anode, and dioxalane mixed with lithium per chlorate as electrolyte. Copper (II) oxide can be used to produce other copper salts. It is also used while welding with copper alloys (Borgohain *et al*., 2002).

CuO is also used as a high capacity electrode material for Li ion batteries and in electronic devices and is also an effective catalyst (Valodkar *et al*., 2011) leading to the complete combustion of organic compounds field emission devices. It is also used as catalysts and sensors. CuO is used in solar energy conversion. It is used as flux in copper and bronze metallurgy, in galvanic electrodes. It serves as solvents for chronic iron ores. It is used to manufacture wood preservatives. CuO nanoparticles are used in gas sensors and acting as an antimicrobial agent and also an antioxidant. Copper (II) oxide can be used to produce other copper salts. It is also used when welding with copper alloys. Another use for cupric oxide is as a substitute for iron oxide in thermite. This can turn the thermite from an incendiary to a low explosive. These advantages make CuO as a suitable compound for new studies to determine its applicability as a material of solar cell, in particular due to its photoconductivity and photoelectric cell properties (Cho, 2013).

2.5.1. CuO Nanoparticles for DSSCs Application

Among the oxides of transition metals, copper oxide (CuO) nanoparticles are of special interest. CuO is a semiconducting material with a narrow band gap and used for photoconductive and photo thermal applications (Onah and Ugwu, 2015). Copper oxide (CuO) is one of the thin films that can easily be deposited on substrates using a simple technique. The first photovoltaic cells observed by Becquerel in 1839 used copper oxide coated metal electrodes immersed in an electrolyte solution. Copper oxide (CuO) is an inexpensive and non-toxic semiconducting material. It is a p-type semiconductor with a narrow band gap (1.2 -1.9 eV), which has interesting photovoltaic, electrochemical and catalytic properties. Copper oxide (CuO) nanoparticles (NPs) are employed as electro catalytic materials for the fabrication of counter electrode in dye sensitized solar cells (DSSCs) (Akinori et *al*., 2005).

2.6. Dye Sensitized Solar Cells (DSSCs)

There are different kinds of photovoltaic's; the traditional silicon solar cells, thin film solar cells, organic solar cells, quantum dot solar cells, perovskite solar cells, and dye-sensitized solar cells that convert solar energy into electricity. For their ease of fabrication, cost, the use of metal oxide

as a non-toxic supporting material and the efficient generation of electricity even at disused (neglected) light conditions dye sensitized solar cells are seems viable one (Willis, 2002).

Grätzel has then extended the concept to the dye sensitized solar cells. The breakthrough for DSSCs occurred in 1991, when Grätzel and O'Regan managed to build a, 7.1%, photovoltaic device based on a dye-sensitized 10 μm thick porous TiO_2 electrode (World Energy Council, 2016). Dye sensitized solar cells (DSSCs) have attracted considerable attention as a potential alternative to the silicon related solar cells. Currently, inorganic solar cell efficiencies range from 30% for multi-junction gallium arsenic solar cells to 20 - 25% for crystalline silicon and thin film to 17% for cadmium telluride. Up to now, optimized DSSC in the liquid electrolyte structure has reached a considerable efficiency of 12.3%. Natural pigment sensitized nanostructured TiO_2 DSSCs have reached an efficiency of 7.1% which is still low compared to the efficiency of Si photovoltaic cells (World Energy Council, 2016).

2.6.1. Operating Principles of DSSCs

Upon illumination of DSSCs the dye absorbs the light leading to excitation of an electron from the higher occupied molecular orbital (HOMO) to the lower unoccupied molecular orbital (LUMO) level. The selected dye is specifically chosen so that the LUMO level is above the conduction band of the metal oxide. As a result the electrons can be injected from the LUMO level of the dye in to the conduction band of the metal oxide leaving a hole behind it (Gratzel, 2005).

The electrons are transported through this layer to the external circuit by electron diffusion and re-enter the cell at the counter electrode. The oxidized dye is regenerated by the reduced species of I/I_3^- redox couple completing, the charge cycle within the cell creating a useful power in the external circuit. The triiodide substitutes the internally donated electron from the external load and reduced back to I^- ion. The movement of electrons in the conduction band of the wide band gap nanostructured semiconductor is accompanied by the diffusion of charge compensating cations in the electrolyte layer close to the nanoparticle surface. Therefore, generation of electric power in DSSC causes no permanent chemical change or transformation (Gong *et al*., 2012).The schematic representation of working principle of DSSCs is shown in Figure 2 below.

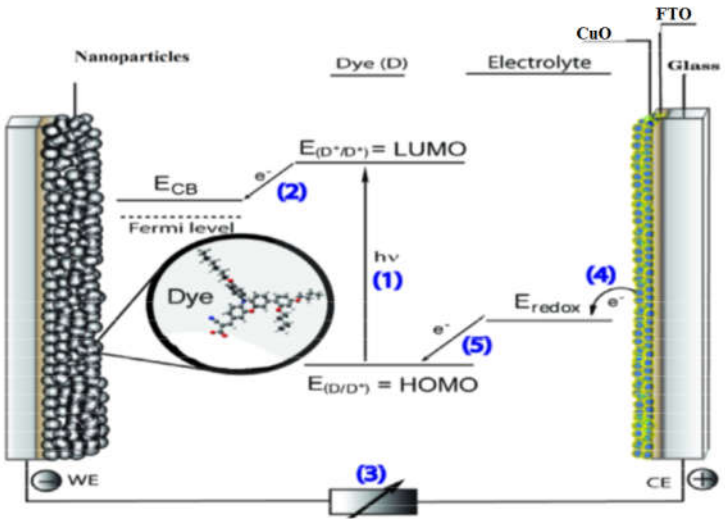

Figure 2. Working principles of dye sensitized solar cell (Gong *et al*., 2012).

As illustrated in Figure 2, the maximum potential produced by the cell is determined by the energy separation between the electrolyte chemical potential (E_{redox}) and the Fermi level of the TiO_2 layer. The small energy separation between the HOMO and LUMO of dye molecule ensures absorption of low energy photons in the solar spectrum. Therefore, the photocurrent level is dependent on the HOMO-LUMO levels separation. In fact effective electron injection into the conduction band of TiO_2 is improved with the increase of energy separation of LUMO and the bottom of the TiO_2 conduction band. Furthermore, for the HOMO level to effectively accept the donated electrons from the redox mediator, the energy difference between the HOMO and redox chemical potential must be more positive (Gratzel, 2005).

2.6.2. Components of DSSC

Dye sensitized solar cells consist of a variety of components. This includes the glass substrate with the transparent conducting oxide (TCO) layer, a mesoporous metal dioxide layer, photo sensitizer (dye), redox couple and a counter electrode.

2.6.2.1. Transparent Conductive Oxide (TCO)

DSSCs are typically constructed with two sheets of conductive transparent materials, which provide a substrate for the deposition of the semiconductor and catalyst, acting also as current collectors. Substrates have to be highly transparent to allow the passage of maximum sunlight to the active area of the cell in order to excite electrons within the DSSC. The electrical conductivity of the substrates should also be high for efficient charge transfer and to minimize energy loss. Typically, FTO and ITO are

widely used as the conductive substrate in DSSCs. It works as a current collector as well as support material and sealing layer for the cell (Tennakone et *al*., 2009).

2.6.2.2. Titanium Dioxide (TiO_2)

Titanium dioxide is a kind of non-toxic inorganic semiconductor with large band gap and chemically stable against corrosion. This large band gap is needed in dye-sensitized solar cell for the transparency of the semiconductor electrode for the wide range of the solar spectrum (Park *et al*., 2000). Semiconductor oxides used in dye sensitized solar cell include TiO_2, ZnO, SnO_2 and Nb_2O_5, among all these semiconductors, nanoporous anatase TiO_2 has been chosen as the standard semiconductor in the DSSCs for its excellent performance. Because it has no photo-degradation phenomena upon excitation compared with other semiconductors which have similar band gap, low cost, easy commercial availability, nontoxicity, and better efficiency achieved in the cell. The role of the nanocrystalline porous oxide is to act as a host for the monolayer of the sensitizing dye molecules using their large surface area and a medium for electron transport to the conducting substrate to produce an electric current (Ardo and Meyer, 2009).

The high conduction band edge energy of TiO_2 leads to higher Fermi level and higher V_{oc} in DSSCs Furthermore, its interesting physical, chemical, and also electron transport properties made TiO_2 material is choice for DSSCs (Ardo and Meyer, 2009).

2.6.2.3. Redox Electrolyte

Redox electrolyte serves to regenerate the dye which has been oxidized by electron injection into the semiconductor and to transfer the reduced charge to the counter electrode, where the reduction - oxidization couple (iodide/tri-iodide) is regenerated by an electron flowing back through the external circuit with the help of the counter electrode layer. The electrolyte consists of redox couple (iodide/tri-iodide) in an organic solvent which is widely applicable in DSSCs due to its stability, diffusion rapidly and low visible light absorption. Iodide (I^-) reduces the oxidized dye and becomes tri-iodide (I_3^-); tri-iodide then moves to the counter electrode and is reduced back into iodide (Macht *et al*., 2002). Hence, the properties of the redox electrolyte should meet the following requirements:

(i) Excellent interfacial properties with both photoelectrode and counter electrode.

(ii) Good chemical, thermal, optical, interfacial and electrochemical stability to prevent degradation of the dye.

(iii) High conductivity to ensure fast charge transfer.

(iv) The electrolyte used in DSSC should have high solubility and high diffusion coefficients in DSSC to ensure efficient charge carriers transport.

(v) It must be highly reversible for fast electron transfer at the counter electrode and be chemically inert toward all other components in the DSSC.

(vi) It should not absorb light strongly at wavelengths in visible region which cause decomposition and unwanted products.

(vii) The electrolyte must regenerate the oxidized dye molecule quickly.

2.6.2.4. Counter Electrode

The oxidized electrolyte diffuses towards the counter electrode where it accepts electrons from the external circuit. A catalyst is required to accelerate the reduction reaction. The standard counter electrode in most works is platinized TCO glass because of platinum has been shown to be a good catalytic activity for the reduction of the redox couple and its high conductivity for charge transport. However, platinum is an expensive material and is not much abundant on earth's crust. For this reason the possibility to substitute this material with cheaper and more available material is an outstanding topic in DSSCs development and industrialization path. It is desirable to substitute a low-cost catalytic material, such other materials are conductive polymers (such as PEDOT), Carbon black, carbon nanotubes, metal oxide and graphene. Among this CuO electrode is known to be a potential alternative to platinum due to its good conductivity, remarkable stability and a comparatively lower price. The electrode showed faster reaction rate and higher electro-catalytic activity for tri-iodide reduction (Murakami *et al*., 2008).

2.6.2.5. Dye Sensitizer

In DSSC, the photosensitizer is one of the most important components influencing solar cell performance, because the choice of sensitizer determines the photo-response of the DSSC and initiates the primary steps of photon absorption and the subsequent electron transfer process. The absorption spectrum of the ideal dye for DSSC should cover the whole visible region and even part of the near-infrared. In addition, the dye must have suitable anchoring groups, which firmly attach the molecule to the semiconductor oxide. The function of the dye sensitizer is to absorb light, inject electrons into the semiconductor conduction band and then accept electrons from the redox mediator in the electrolyte. The most efficient sensitizers in nanocrystalline TiO_2 DSSC are based on polypyridyl complexes of

transition metals, particularly ruthenium based dye (Mary and Rosana, 2015). This is because they show a strong and broad absorption band in the visible range and rapid charge injection rates. These complex dyes are capable of delivering DSSCs with high conversion efficiencies. However, its high cost, long-term unavailability, heavy environmental burden and complicated synthesis are major drawbacks of using these complex dyes. As a result metal-free organic dyes have also received intensive research interest as promising sensitizers in DSSCs owing to their high molar extinction coefficient, cost-effective synthesis processes as compared with Ru based dye and high flexibility of the molecule structures . But these Ru based synthetic dyes have been still problems, such as complicated synthesis routes. Currently natural dyes have also been used in DSSCs because of their low cost, easy extraction, nontoxicity, readily available and the environmentally benign nature. They provide available alternative to expensive ruthenium metal based DSSCs (Murakami and Grätzel, 2008).There are four classifications of natural plant pigments: chlorophyll, carotenoids, anthocyanins and betalains; all of which have been used in natural pigment sensitized DSSCs to varying degrees.

Chlorophyll derivatives

Chlorophyll is the major light-absorbing pigment in green plants. It is located within the membrane of the chloroplasts, which are small, green organelles which initiates photosynthesis by absorbing energy from sunlight and transferring this energy to other molecules. Chlorophyll has magnesium as its central metal ion, and the large organic molecule to which it bonds is known as a porphyrin. The porphyrin contains four nitrogen atoms bonded to the magnesium ion in a square planar arrangement (Mary and Rosana, 2015). Chlorophyll occurs in a variety of forms but plants contain chlorophyll a and b. These two types of chlorophyll differ only slightly, in the composition of a side chain. Both of these two chlorophylls are very effective photoreceptors because they contain a network of alternating single and double bonds, and the orbital's can delocalize stabilizing the structure. Such delocalized polyenes have very strong absorption bands in the visible regions of the spectrum, allowing the plant to absorb the energy from sunlight (Ludin, 2014). Chlorophyll absorbs light in the red (long wavelength) and the blue (short wavelength) regions of the visible light spectrum. Green light is not absorbed but reflected, making the plant appear green. But even if chlorophyll absorbs most of the blue and red light, the accessory pigments known as carotenoids can serve to enhance the absorption in the blue-green and yellow part of the spectrum.

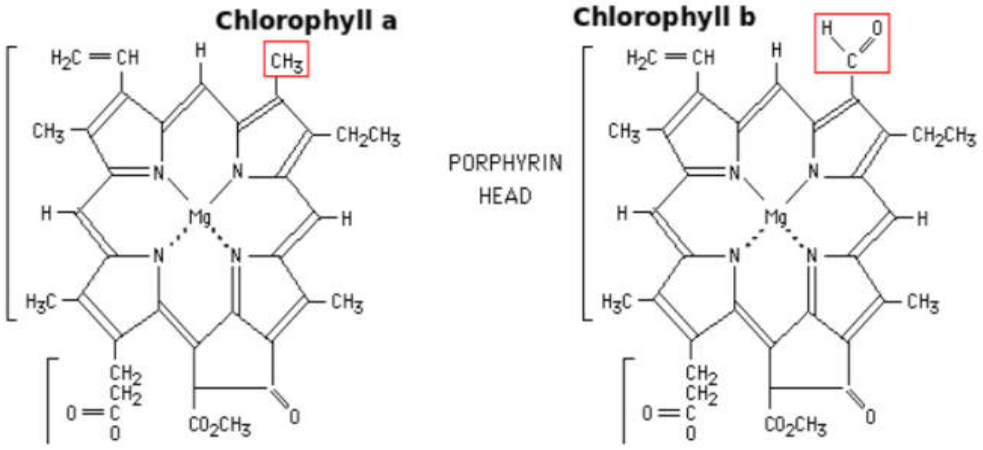

Figure 3. Structure of chlorophyll a and b.

In nature, carotenoids also act as energy transfer molecules for chlorophyll and prevent degradation of the molecules by quenching certain energy states, thus acting as photo protectors. Another interesting feature found in nature is the stacking of the thylakoidmembranes (containing the chlorophyll) to enhance light absorption. Such stacking has similarities with the structure of the mesoporous network in a DSSC. These properties make photosynthetic pigments attractive to use as sensitizers in solar cells. As mentioned before, these molecules become cation radicals and are susceptible to undesirable side reactions before being reduced by the electrolytic species (Baker, 1996)

Anthocyanin

Anthocyanin is one of flavonoid compound present in many fruits, flowers; leaves and is responsible for the red, blue, violet, orange and pink colors (Ludin, 2014). It has been reported to exhibit anti-oxidant and anti-cancer properties. The presence of the carbonyl and hydroxyl functional groups in the structure of anthocyanin helps an excess anchoring of the dye on the surface of TiO_2 film and also causes an easy electron transfer from the anthocyanin molecule to the conduction band of TiO_2 (Ludin, 2014). Moreover, it can display colors in the visible region from red to blue that makes them an efficient photo sensitizer and vital alternative for synthetic dyes, and most of other natural sensitizer. The maximum absorption of anthocyanin extracts ranges from 510 to 548 nm depending on the fruit, leaves and flowers or the solvent used (Chappel, 2005).

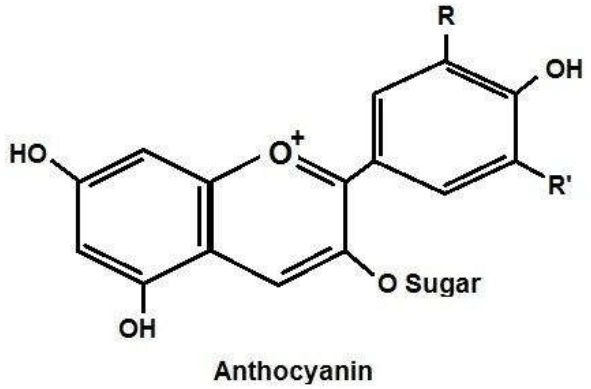

Figure 4. Chemical Structure of Anthocyanin

Betalains

Betalain pigments represent an additional class of organic natural dyes of potential interest, they were extracted from beets and their name is even based on the word beet. These pigments are present in caryophyllale plants, have high molar extinction coefficients in the visible region and pH dependent redox properties. The pigments are present in the different parts of the plant including flowers petals, fruits, leaves, stems and roots.

The two main types of betalains that are present in plants are betcyanins and betaxantnines which absorb light differently and give a different spectrum of color to the plants. Within these 2 categories, many subcategories are present. Betacyanins which are the reddish to violet betalain pigments, and betaxanthins which are the yellow to orange betalain pigments. Figure 5 shows the the two types of betalains (Longo and De Paoli, 2003).

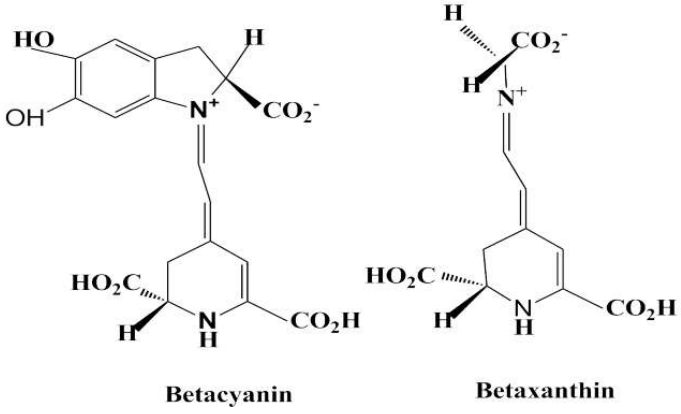

Figure 5. General structure of betalains: betcyanin and betaxanthin

Synthetic dyes

Originally, a dye was defined as an organic compound (i.e., one that contains the element carbon) that emitted a brilliant color when exposed to visible light. This color could be imparted to other materials such as cloth, which was then said to be "dyed."Today this definition has been broadened to include hundreds of organic compounds with certain chemical ingredients and behavior in absorbing and emitting light. Thus, for example, dyes may be colorless and may absorb and emit not only in the visible spectrum but also in the ultraviolet and near infrared (Cremurs, 1977).

Crystal violet (CV) is try-aryl-methane dye whose chemical structure is shown in Figure 6. It is used as acidic-base indicators and stain compounds in histology. It is one of the fluorescent dyes which absorb and emit light in the visible region of spectrum. The optical investigation of thin film of this dye constitutes an important tool to enhance its applications in optical filter, display device and solid state photovoltaic cell.

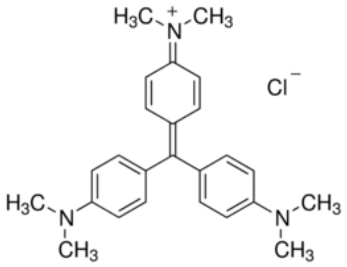

Figure 6. Structure of crystal violet dye

Generally pigments appear colorful because they selectively reflect and absorb certain wavelengths of visible light. White light is a roughly equal mixture of the entire spectrum of visible light with a wavelength in a range from about 380 or 400 nm to about 760 or 780 nm. When this light encounters a pigment, parts of the spectrum are absorbed by the chemical bonds of conjugated systems and other components of the pigment. Some other wavelengths or parts of the spectrum are reflected or scattered. Most pigments are charge-transfer complexes, like transition metal compounds, with broad absorption bands that subtract most of the colors of the incident white light.

2.5.3. Characteristics of DSSCs

The solar cell performance is determined using its current-voltage (J-V) characteristics under standard illumination conditions (Meidan *et al*., 2015). Figure 7 shows characteristic J-V curve of a DSSCs system.

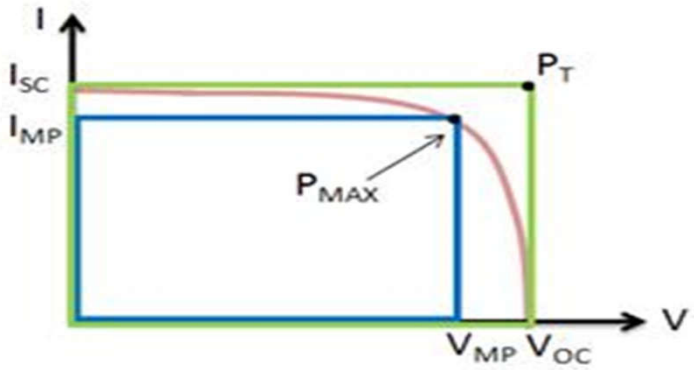

Figure 7. Characteristic J-V curve of a DSSCs system (Macht *et al*., 2002).

i. Short Circuit Current Density (J_{sc}): The short-circuit current density is the maximum current from a cell and occurs when the voltage across the device is zero, the cell is said to be short circuited and the current is called short circuit current. It is due to the generation and collection of light-generated carriers.

ii. Open Circuit Voltage: The open-circuit voltage (Voc) is the maximum voltage available from a solar cell and is achieved when there is no photo-generated current (I_{sc}= 0). It is determined by the difference between the redox potential of the electrolyte and the bottom of the conduction band of working electrode materials. It can be calculated by:

$$V_{OC}=\frac{nkT}{q}\ Ln(\frac{Iph}{I_o}) \qquad (1)$$

Where, n is ideality factor of the diode (for an ideal diode n=1),k is Boltzmann constant, T is absolute temperature, q is charge on an electron, I_o is the inverse saturation current density and I_{ph} is photo generated minority carrier current and equals to the product of absorbed photon flux and the charge on an electron.

iii. Maximum Power Point (P_{max}): Maximum power is the product of the maximum current (I_{max}) and maximum voltage (V_{max}). Where: maximum current (I_{max}), it is the current at the optimum operating

point at which the DSSC output power is maximum and, maximum voltage (V_{max}), it is the voltage at the optimum operating point at which the DSSC output power is maximum.

iv. **Fill Factor (FF)**: The fill factor (FF) is a measure of the maximum power output from a solar cell with reference to a hypothetical maximum power (J_{sc} x V_{oc}). It depicts the squareness of the IV curve and reflects the extent of electrical & electrochemical losses during cell operation of DSSCs.

Mathematically it can be determined by:

$$FF = \frac{J_{max} . V_{max}}{J_{SC} \cdot V_{OC}} \qquad (2)$$

v. Power Conversion Efficiency (η): A DSSC energy conversion efficiency (η) is the percentage of power converted (from absorbed light to electrical energy) and collected when a solar cell is connected to an electrical circuit. It can be determined by dividing P_{max} by the total incident light power, P_{in} in the I-V curve.

$$\eta = \frac{Jsc . Voc . FF}{Pin} \qquad (3)$$

Where P_{max} - is maximum output power and P_{in} - is the power of incident light, J_{sc} &V_{oc} are short circuit current density & open circuit voltage respectively.

vi. Incident Photon to Current Conversion Efficiency (IPCE)

IPCE is one of the fundamental measurements of the performance of solar cell. It is also known as the external quantum efficiency and describes how efficiently the light of a specific wavelength is converted to current that is (electrons out) / (photons in). The IPCE can be calculated according to equation (Vahermaa *et al*., 2010).

$$IPCE\ (\%) = \left(\frac{1240.\ Jsc}{\lambda.\ Pin}\right).100 \qquad (4)$$

J_{sc} is the short circuit current density, λ is the wavelength of the incident light and P_{in} is the intensity of the incident light.

3. MATERIALS AND METHODS

3.1. Collection of Plant Material

Fresh leaves of khat (*Catha edulis*) and *kniphofia schemperi* root were collected from Bedesa Woreda East Arsi zone Oromia region, 120 km from Adama city and Bale Mountains National Park, Oromia Region, Bale zone, Ethiopia, respectively.

3.2. Chemicals and Reagents

Copper (II) nitrate trihydrate (UNI-CHEM Chemical Reagents), Sodium hydroxide (Alkem Industry & Trading), Acetone (Aldrich), 2-Propanol (Riedel-de Haen) and Ethanol (Fluka), TiO_2 nanopowder (30% rutile and 70% anatase, Sigma Aldrich), Triton X-100 detergent (Aldrich), FTO, 15 Ω/sq, (Sigma Aldrich), 35% (w/w) of PVP (polyvinylpyrolidone)(Sigma Aldrich)),Acetonitrile (Sigma Aldrich), Iodine (Sigma Aldrich)1-ethylene-3-methylimmidazolium iodide ((EMIM-I) Aldrich), Nitric acid and Sodium iodide (Sigma Aldrich).

3.3. Apparatus and Equipments

In this study different apparatus and instruments were used such as:- thermo gravimetric analysis (TGA-DTA), FTIR, XRD, UV-Vis spectrophotometer, SEM-EDX, TEM, digital electronic balance, oven, furnace, electronic centrifuge, ultrasonic bath, glass filters, computer controlled electrochemical analyzer (CHI630A), test tube, borosilicate glass, magnetic stirrer, mortar and pestle, cylindrical glass, pH meter, micro grinding machine, hot plate, micropipettes, spatulas, Erlenmeyer flask, volumetric flask, different types of beakers, plastic bottles, aluminum foil, towels and many others were used.

3.4. Preparation of Plant Leaf Extracts

First, the leaves were washed with distilled water to remove the dust particles. After that the leaves were dried in 7 days at room temperature and then ground into a fine powder using mortar. 10 g of *Catha edulis* powder was taken for synthesis purpose and boiled with 150 mL of distilled water for 30 min at 80 °C until the color of the aqueous solution changes from watery to light brown. The extract was cooled at room temperature and filtered by Whatman №1 filter paper, and the extract was stored in a refrigerator at 4 ^{0}C in order to be used for further studies (Naika *et al*., 2015).

3.5. Synthesis of CuO Nanoparticles Using *Catha edulis*

Copper (II) nitrate trihydrate, Sodium hydroxide, Distilled water and *Catha edulis* leaves extract were used for the synthesis of CuO NPs. Copper (II) nitrate trihydrate was used as precursor to synthesize CuO nanoparticles using aqueous extract of *catha edulis* leaf and 1 M of NaOH were prepared and used as a precipitating agent. Then three different samples were prepared with different ratios by taking different weight of precursor salt and volume of *catha edulis* leaf extract by using the method developed by (Jitendra *et al*., 2015). For each sample 100 mL plant leaf extract was taken and heated at 80 °C while stirring using magnetic stirrer. Measured amount of precursor salt was added after the solution temperature reached 80 °C.

Sample 1:- 10 g of Cu $(NO_3)_2 3H_2O$:100 mL *catha edulis* leaf extract ratio (1:10) labeled as **CuO (1:10)**
Sample 2:- 30 g Cu $(NO_3)_2 3H_2O$: 100 mL *catha edulis* leaf extract ratio (3:10) labeled as **CuO (3:10)**
Sample 3:- 50 g Cu $(NO_3)_2$ $3H_2O$: 100 mL *catha edulis* leaf extract ratio (1:2) labeled as **CuO(1:2)**

Then for each sample the mixture was stirred continuously with magnetic stirrer at 80 **°**C until the color changes from deep green to deep brown precipitate observed. The precipitate was centrifuged at 1000 rpm for 30 min and washed with deionized water and again centrifuged for 20 min in order to remove the impurities. Finally, the precipitate was dried in an oven at 150 $^{\circ}$C for 3:30 hrs and was ground to fine powder using agate mortar. The black powder obtained from the above method was calcined at 400 ^{0}C for 2 hour.

3.6. Characterization of CuO Nanoparticles Using TGA-DTA

Thermal gravimetric analysis (TGA) was carried out using a simultaneous TGA-DTA apparatus (DTG-60H, Shimadzu Co., South Korea) to determine the calcinations temperature of the synthesized material. About 10.531 mg of the uncalcinated CuO nanoparticle sample was placed in a platinum crucible on the pan of the microbalance and heated from room temperature to 1000 °C, using Al_2O_3 as inert material.

3.7. Characterization of CuO Nanoparticles Using XRD

The synthesized CuO NPs were characterized by using X-ray diffraction (XRD) characterization technique (Shimadzu XRD 6000).XRD was carried out with scan range 10 - 80° with using Cu Kα radiation (λ = 1.5406 Å) while the accelerating voltage and applied current is held at 40 kV, 30 mA

respectively with scan rate 0.02° s^{-1}(Ruiz *et al*., 2015). The particle size of the powders was calculated by using Scherer's Formula;

$$D = \frac{K\lambda}{\beta cos\theta} \qquad (5)$$

Where, d is crystallite size in nanometer, k is shape factor constant, which is 0.89, β is the full width at half maximum (FWHM) in radian, λ is the wave length of the X-ray and θ is the Bragg angle.

3.8. Characterization of CuO Nanoparticles Using SEM-EDX

The morphological feature of the synthesized CuO NPs was analyzed using Scanning Electron Microscopy (FE-SEM, JEOL-GSM 6500F, JAPAN), using electron beam energy of 20 KV with tilt angle 45 °C. The CuO NP powder was mounted on a sample holder followed by coating with a conductive metal. Then, the sample was scanned with focused fine beam of electrons. The surface characteristics of the sample were obtained from the secondary electrons emitted from the sample surface.

The elemental analysis or chemical composition of the synthesized powder was done by using energy dispersive Spectroscopy (EDX) at the Electron Microscope Unit (EMU). To prepare the sample small amount of the synthesized powder was scooped and placed in the pellet maker. The prepared pellet was then coated with carbon before mounting in the machine. Then the powder was compressed with a high pressure. The operation was done at excitation energy of 20 K eV with scan or acquisition time of 600 second (Ruiz *et al*., 2015)

3.9. Characterization of CuO Nanoparticles Using TEM

Transmission electron microscopy (TEM) also sometimes called conventional transmission electron microscopy or CTEM) is a microscopy technique in which a beam of electrons is transmitted through a specimen to form an image of the sample (Ruiz *et al*., 2015). The biosynthesized CuO nanoparticles were analyzed by using high-resolution transmission electron microscope (HRTEM, Tecnai F20 G2, Philips, Netherlands) at an accelerating voltage of 200 kV.

3.10. Characterization of CuO Nanoparticles Using UV-Vis Spectroscopy

The optical absorption spectra of the synthesized CuO NPs were determined using UV/Vis spectrophotometer (JASCO V-670 UV-Vis spectrophotometer equipped with a diffuse reflectance

attachment for powder samples). The solid state absorbance of the synthesized CuO was measured by scanning over the wavelength range of 200-900 nm (Mohanpuria *et al*., 2008).The ASCII files of the measured spectra were collected by computer which interfaced with the instrument.

3.11. Characterization of CuO Nanoparticles Using FT-IR

The synthesized CuO nanoparticles were characterized by Fourier transform infrared spectroscopy (PerkinElmer, Spectrum 65 FTIR) in order to analyze and detect surface functional groups at the scanning range of 4000 – 400 cm^{-1}. For the FT-IR characterization, the sample was mixed with solid KBr uniformly and properly, which was compressed to settle down on a thin transparent film and this thin transparent film was for FT-IR analysis which was kept in the chamber of the instrument for scanning.

3.12. Fabrication and Characterization of DSSCs

❖ Preparation of Natural pigment and Crystal Violet Dye

After collection, the plant *kniphofia schemperi* was dried under shade area for two months at room temperature to protect degradation of pigment. After that the sample was crushed using electrical supper blender to produce a fine powder. This powder was used for extracting dye with ethanol solvent. Two gram of a powdered sample was taken and soaked in 50 mL of ethanol for dye extraction in a flask. The solutions were stirred for 2 hours by using a magnetic stirrer, and kept for 24 hours including the stirring time to disperse the powder completely and stored at room temperature. Then the solution was filtrated by decantation followed by a glass filter to obtain clear dye solution and put with a glass bottles covered with aluminum foils to prevent damage from light exposure (Murakami and Grätzel, 2008). And 0.001M of the crystal violet dye were prepared by taking 0.102 gram of powder crystal violet dye and dissolved in 250 mL volumetric flask by using distilled water. And the solution was shaken continuously to facilitate the reaction and filled the flask until the mark reaches.

❖ Preparation of the Substrate for Deposition

Fluorine doped tin glass (FTO) (1.5×1.5 cm) substrates were cleaned using acetone, 2- propanol and ethanol solvents for 20 minutes using ultrasonic bath and air dried before use.

❖ TiO_2 Nanoparticles Paste Preparation and Deposition

1.5 g of commercial TiO_2 nanopowder was ground in a porcelain mortar with 1 mL H_2O containing 1 $MHNO_3$ to prevent reaggregation of the nanoparticles. After the powder had been dispersed by the high shear forces in the viscous paste, it was diluted by slow addition of 2 mL water under continued grinding. Finally 0.05 mL Triton X-100 detergent was added to facilitate the spreading of the colloid on the substrate.

The simplest and most widely used method for depositing TiO_2 paste on a substrate is the doctor blade method. The technique is also known as slot-coating in its mechanized version. It uses a hard squeegee, or doctor-blade, to spread a portion of TiO_2 nanoparticles paste onto the glass Which was applied by: 1st the FTO coated side of the substrate (conductive side) faced up; secondly, small portion on the four edges of the substrate was covered by using scotch tape and made ready for covering TiO_2 nanoparticles paste. After making the paste ready for deposition, the paste was applied on uncovered portion of FTO and coated with the help of a glass rod and the paste was spread across the active plate. The preparation of electrode was completed by firing (sintering) the deposited layer at 450 °C for 30 minutes after removing the scotch tape. The organic solvent burns away, leaving the TiO_2 nanoparticles sintered together. This process ensures electrical contact between particles and good adhesion to the FTO glass substrate.

- **Electrode Sensitization**

Before immersion in the pigment solution, films were warmed at (80°C) to minimize the water vapor content inside the porous of TiO_2 nanoparticles film. The sensitization was performed at room temperature for 12 hours. The best method of adsorbing a natural sensitizer to the oxide layer is by dipping the electrode in a solution of the natural pigment already extracted/prepared. After sensitization, the films were rinsed with the same solvent (ethanol, distilled water) used to prepare the pigment solution (Murakami and Grätzel, 2008).

- **Preparation of Redox Electrolyte**

The polymer gel electrolyte was prepared according to the method described below (Meidan *et al*., 2015). 0.9 M of 1-ethylene-3-methylimmidazolium iodide (EMIM-I) and 0.5 M NaI were prepared by using the solvent acetonitrile (high dielectric constant organic solvent) in a separate volumetric flask and mixed to form a solution. After that 0.5 M of sodium iodide solution was added into the above solution under stirring to form a homogeneous liquid electrolyte and in order to obtain a better conductivity. Then 0.12 M iodine and 35% (w/w) of PVP (polyvinylpyrolidone) (0.54 g of PVP) were added. Then,

the resulting mixture was heated at 70-80 °C under vigorous stirring to dissolve the PVP polymer, followed by cooling down to room temperature to form a gel electrolyte.

❖ Coating Counter Electrodes

0.5 g of black powder of each synthesized CuO NPs was added in ethanol in different crucibles. After the powder was dispersed by the high shear forces in the viscous paste and few drops of Triton-X100 were added in to the paste preparation to disperse the colloid on the substrate. Afterward, CuO NPs paste was deposited on the cleaned fluorine doped tin oxide (FTO, 8 Ω/sq, 80% transmittance in the visible light) glass by simple casting method using glass rod at room temperature. After natural dry, the CuO NPs deposited FTO glass substrates were heated at 250 °C for 15 min to remove the organic solvents and contaminants and CuO NPs based counter electrode was prepared (Murakami and Grätzel, 2008).

❖ Device Assembly and Characterization

Device assembly is the final step for characteristics measurement. Here the sensitized electrode was washed by the solvent of the dye and dried using hair dryer to dry the electrode, and then the non-covered part of the film by the paste was covered by a tape spacer in all side by leaving some place for electrical contact. By facing the active sides of the photoanode and the cathode, the two electrodes were pressed together after putting the quasi electrolyte on the photoanode.

Then the devices were made ready for characterization. The photoelectrochemical measurements of the solar cells were performed using a computer controlled CHI630A Electrochemical Analyzer. A150-W Xenon lamp regulated by an Oriel power supply (Model 68830) was used to illuminate the DSSCs. A grating monochromator (Model 77250) placed into the light path was used to select a wavelength between 300 and 800 nm. The intensity of the incident light was set to be 100 $mWcm^{-2}$ using optometer. The DSSCs solar cell was then mounted in a sample holder inside a metal box with an area of 1 cm^2 opening to allow light from the source. All experiments were carried out at ambient temperature.

4. RESULTS AND DISCUSSION

4.1. Synthesis of CuO Nanoparticles

The CuO NPs was synthesized by reaction between *Catha edulis* leave extract and solid copper nitratetrihydrate precursor up on mixing. *Catha edulis* was used to reduce the copper ions (Cu^{2+} to Cu^{0}).Upon continuous heating of the mixture, green solution of the plant extract slowly turned into darker green colored solution followed by formation of brown precipitate that is one of the confirmations of formation of CuO nanoparticles by reduction reaction.

$$Cu\,(NO_3)_2.\,3H_2O + \text{Plant extract} + 2NaOH \rightarrow CuO + 2NaNO_3 + 4H_2O + \text{byproducts}$$

In this study, green synthesis of CuO NPs was successfully accomplished by using *catha edulis* leaf extract. It was reported that *Catha edulis* contains a lot of chemical components such as: alkaloids, terpenoids, flavonoids, sterols, glycosides, tannins, amino acids, and vitamins and minerals (Lamina, 2010). These and other chemical constituents of *Catha edulis* leaf extract made *Catha edulis* to be used as a reducing and capping agent in synthesis of nanoparticles. This greener approach was exploited as it is easier to be carried out without any complicated experimental procedure. In addition, these methods are comparatively low cost as natural agricultural plant scan be utilized and are free of non-green solvents (Ibrahim H., 2015).

4.2. Characterization of CuO NPs

4.2.1. Thermal Gravimetric Analysis (TGA-DTA)

The uncalcinated CuO nanoparticles synthesized was characterized using TGA/DTA.

Figure 8 shows the thermal gravimetric analysis/differential thermal analysis (TGA/DTA) data of the given synthesized copper oxide nanoparticle. TGA curve shows mass loss of the sample whereas DTA curve indicates the energy gain or loss during the process. The TGA curve showed a three-step decomposition of the uncalcined nanoparticle. During thermal treatment of the synthesized nanoparticle, mass losses were observed in the temperature range 25 -150 °C, 400-600 °C, and 601-1000 °C. The weight loss of the material observed between the temperatures 25-150 °C was about 11.594% that could be due to vaporization of water content in the material. The weight loss observed in the temperature range of 400-600 °C was about 1.35% that is most probably due combustion of organic compounds

from *catha edulis* extract. The weight loss above temperature of 600 °C which was about 2.626% may be due to oxygen loss (Aparna *et al*., 2016).

Generally, the total weight loss of the synthesized CuO nanoparticles observed from TGA was about 15.570% which was not significant and indicates the thermal stability and also good purity of the synthesized nanoparticles. Accordingly, the calcinations temperature was selected to be 400 $^{\circ}$C beyond which the mass loss of the NPs was very insignificant until the temperature reaches 600 $^{\circ}$C. The results revealed that the nanoparticles calcined at 400 °C consist of CuO monoclinic structure and monoclinic distortion decreases with increasing calcination temperature up to 1000 °C then increased with increasing temperature. Some researchers reveled that another phase Cu_2O was formed instead of CuO in the transition sequence from the Cu^{+2} to Cu^{+1} phase to calcinate above 500 °C (Aparna *et al*., 2016).

The TGA curve shows some little mass loose until 1000 °C this mass loose comes from undecomposed plant materials. This undecomposed molecules confirmed by the FTIR spectrum like amine groups (1383 cm^{-1}), phenolic groups (2875 cm^{-1}) and alcoholic groups (3439 cm^{-1}). This molecules coated on the surface of the nanoparticle due to this if we calcined above the temperature 500 °C the synthesized CuO NPs may change the phase due to his the calcination temperature were selected at 400 °C.

The chemical decomposition with an increase of temperature was examined through DTA and it appeared as the endothermic and exothermic peaks in the DTA curve. On the basis of both the prevailing conditions, the weight loss indicated dehydration of the sample, In other words, it meant loss of free and coordinated water molecules up to 110 $^{\circ}$C from the sample. The result in the second stage was primarily consequent to the thermal decomposition noticed at around 150, 250 and 350°C shows high weight loss and high exothermic peak. And endothermic peaks could be observed with the DTA curve in the temperature around 190 and 400^{o}C under the previous conditions.

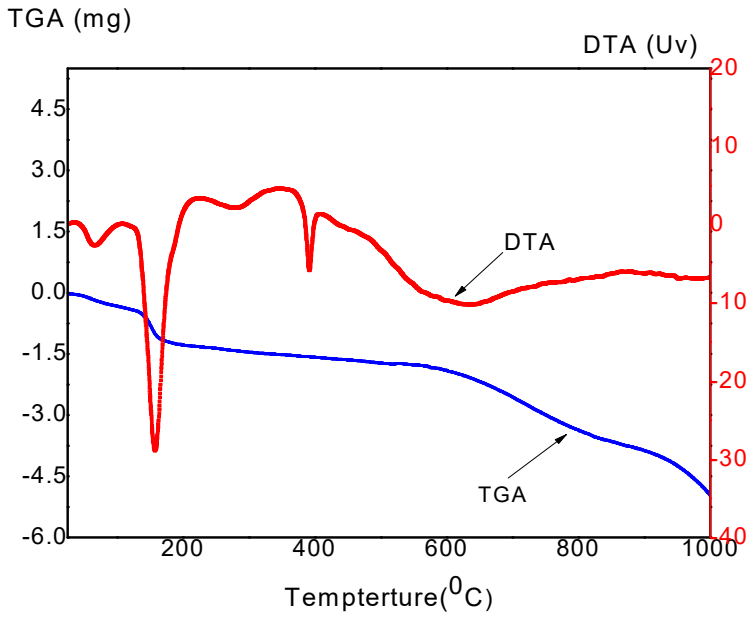

Figure 8.Thermal Analysis result for uncalcinated 1:10 ratio copper oxide nanoparticles

4.2.2. X-Ray Diffraction (XRD)

The CuO NPs biosynthesized from *Catha edulis* leaf extract were confirmed by the characteristic peaks observed in the XRD patterns as shown in Figure 9 a, b and c with 1:10, 3:10 and 1:2 weight/volume ratios of precursor and plant extract, respectively.

XRD analysis for 1:10 ratio Figure 9 a shows intense peaks at 31.4876°, 35.4894°,38.6974°, 48.7540°, 53.4330°, 58.2323°, 61.5322°, 66.2470°, 67.6419°, 72.3621° and 75.2398°, corresponding to miller indices of (110), (002), (111), (202), (020), (202), (113), (311), (113), (311) and (222) respectively. The sharp and narrow diffraction peaks indicating highly crystalline structure nature and also phase purity of nanoparticles. The lattice parameters of CuO sample were calculated from the XRD data. The evaluated cell parameters were a = 0.46891 nm, b = 0.34214 nm, and c = 0.51276 nm in agreement with the reported values. Table 1 summarizes the diffraction pattern and miller indices of 1:10 ratio synthesized CuO NPs.

Table 1. The diffraction pattern and miller indices of 1:10 ratio synthesized CuO NPs

Peak №	2θ Value (degree)	FWHM Value	Miller indices (hkl) Value
1	31.4876	0.3037	110
2	35.4894	0.2782	002
3	38.6974	0.3276	111
4	48.754	0.3058	202
5	53.433	0.3145	020
6	58.2323	0.3411	202
7	61.5322	0.3098	113
8	66.247	0.3451	311
9	67.6419	0.216	113
10	72.3621	0.2936	311
11	75.2398	0.2542	222

The observed diffraction reflections are comparable with JCPDS № 048-1548 and are attributed to bulk CuO materials. All diffraction peaks can be indexed as the typical monoclinic structure and no extra diffraction peaks of other phases are observed. Moreover, the well-defined and sharp CuO reflections in the observed XRD patterns verify the well-crystalline nature of CuO NPs. Similar result was obtained by (Jitendra *et al.*, 2015).The crystalline size of the CuO NPs was calculated using Debye Scherer equation. As a result, the crystalline size of CuO NPs corresponds to the highest intense peaks was calculated to be 28.10 nm.

Figure 9 b shows 3:10 ratio of the XRD pattern of synthesized CuO NPs. The observed diffraction peaks at 2θ = 32.4911°, 35.5036°, 36.4007°, 38.4007°, 48.8047°, 53.4321°, 58.2223°, 61.5010°, 65.7825°, 67.9854°, 72.3607° and 75.7198° corresponding to (110), (002), (111), (202), (020), (202), (113), (311), (113), (311) and (222) crystal planes, respectively. The sharp diffraction peaks in the XRD pattern distinctly depict the crystalline nature of the sample (Sankar *et al*., 2014). Table 2 summarizes the diffraction pattern and miller indices of 3:10 ratio synthesized CuO NPs.

Table 2. The diffraction pattern and miller indices of 3:10 ratio synthesized CuO NPs

Peak №	2θ Value (degree)	FWHM Value	Miller indices (hkl) Value
1	32.4911	0.279	110
2	35.5036	0.3189	002
3	38.4007	0.2908	111
4	48.8047	0.3394	202
5	53.4321	0.4393	020
6	58.2223	0.4429	202
7	61.501	0.4441	113
8	65.7825	0.66	311
9	67.9854	0.4845	113
10	72.3607	0.3167	311
11	75.7198	0.3626	222

The standard diffraction peaks representing the crystal structure of CuO is monoclinic structure according to the standard JCPDS data card № 048-1548. Another two peaks was observed at 2θ=36.4° and 44.9° (with reference to ICSD file no. 98-015-4604) indicating the existence of the Cu_2O at the surface. This may comes to the annealing temperature of the samples in the furnace because the furnace was hot starting to anneal and not increasing gradually due to this, two peaks was observed which consists of cuprites (Cu_2O) phase. There is no tenorite (CuO) phase present at this temperature but only pure cuprites (Cu_2O) phase and it does not affect the composition of the NPs. This behavior can be explained as some copper atoms will bond with oxygen atoms to form Cu_2O as the first oxide phase. This oxidation could be referred by the following reaction: $2Cu + ½\ O_2 \rightarrow Cu_2O$. With increasing in annealing temperature to 400 ^oC, tenorite (CuO) phase started to be appeared and XRD pattern shows an extra peak near 2θ = 38.4° which matches the reflection from (110) plane of CuO. Similar result were obtained by (Faheem *et al.*, 2017). The mean grain size of the CuO nanoparticles was 25.30 nm. This was calculated from the three most intense peaks using Debye-Scherer's formula (Sankar *et al*., 2014).

Figure 9 c shows the XRD pattern of synthesized CuO NPs for 1:2 ratios. XRD pattern displayed that most of the diffraction peaks at 2θ values 31.6751°, 35.5086°, 38.7159°, 48.8047°, 53.4321°, 58.2223°, 61.5010°, 66.2656°, 67.4820°, 72.3607° and 75.2598° were assigned to miller indices of (110), (002), (111), (202), (020), (202), (113), (311), (113), (311) and (222), respectively. Table 3 summarizes the diffraction pattern and miller indices of 1:2 ratio synthesized CuO NPs.

Table 3. The diffraction pattern and miller indices of 1:2 ratio synthesized CuO NPs.

Peak №	2θ Value (degree)	FWHM Value	Miller indices (hkl) Value
1	31.6751	0.3297	110
2	35.5086	0.4075	2
3	38.7159	0.5311	111
4	48.8047	0.4763	202
5	53.4321	0.5347	20
6	58.2223	0.5256	202
7	61.501	0.5019	113
8	66.2656	0.56	311
9	67.482	0.376	113
10	72.3607	0.5783	311
11	75.2598	0.6333	222

The sharp and narrow diffraction peaks indicating highly crystalline structure nature and also phase purity of nanoparticles. The XRD patterns of synthesized CuO NPs were closely matched with the standard data JCPDS card № 048-1548 suggesting that a monoclinic (tenorite) phases crystalline structure. Similar result was obtained by (Rao and Venkatarangaiah, 2014). As a result, the crystalline size of CuO NPs corresponds to the highest intense peaks was calculated to be 18.20 nm.

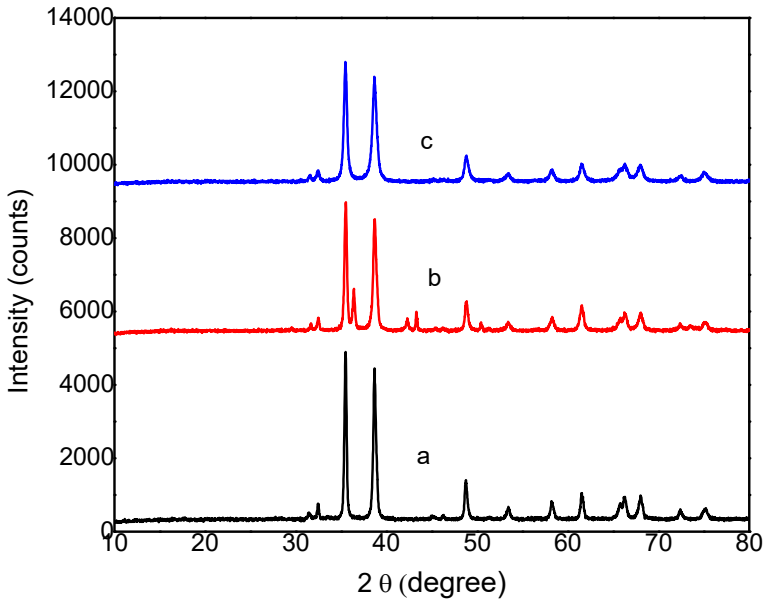

Figure 9. XRD patterns of (a) 1:10, (b) 3:10 and (c) 1: 2 ratios of green synthesized Copper oxide NPs.

4.2.3. Scanning and Transmission Electron Microscopy

The surface morphology and micro structures of CuO NPs were investigated by using SEM analysis as shown in Figure 10 a, b and c. Figure 10 a shows SEM image for 1: 10 ratio of the synthesized CuO NPs which showed uniform and define spherical morphology. It is noticed that green synthesis of CuO NPs produced small and uniform size of spherical particles which is in agreement with previous result reported (Jitendra *et al*., 2015).

Figure 10 b shows SEM image of 3: 10 ratio of the green synthesized copper oxide nanoparticles. Similar to the 1:10 ratio, the SEM image showed spherical shaped CuO NPs but with some aggregation that could be due to the low concentration of the plant extract that acts as capping agent in addition to reducing agent. The spherical of the synthesized CuO NPs is also in agreement with the previous literature report (Mahmoud *et al*., 2015).

Figure 10 c also shows SEM image of 1: 2 ratio of the synthesized copper oxide NPs. The SEM image is similar to the 1:10 ratio. It clearly showed that the particles are small and uniformly distributed over the surface with low aggregation. The low aggregation could also be due to the high fraction of plant extract used which acts as capping/stabilizing agent (Sundaramurthy *et al*., 2015).

Figure 10 d shows the TEM images of synthesized CuO NPs. The low magnification TEM image reveals almost similar spherical morphology of CuO NPs as seen in SEM image. From TEM image which is consistent with the SEM results. From the TEM image of CuO NPs as shown in Figure 10 (d), the particles are aggregated and interconnected to each other, resulting in the less visible lattice fringes. Therefore, the morphological characterizations confirm the spherical morphology of CuO NPs biosynthesized from the leaves of *catha edulis* plant (Jitendra *et al*., 2015).

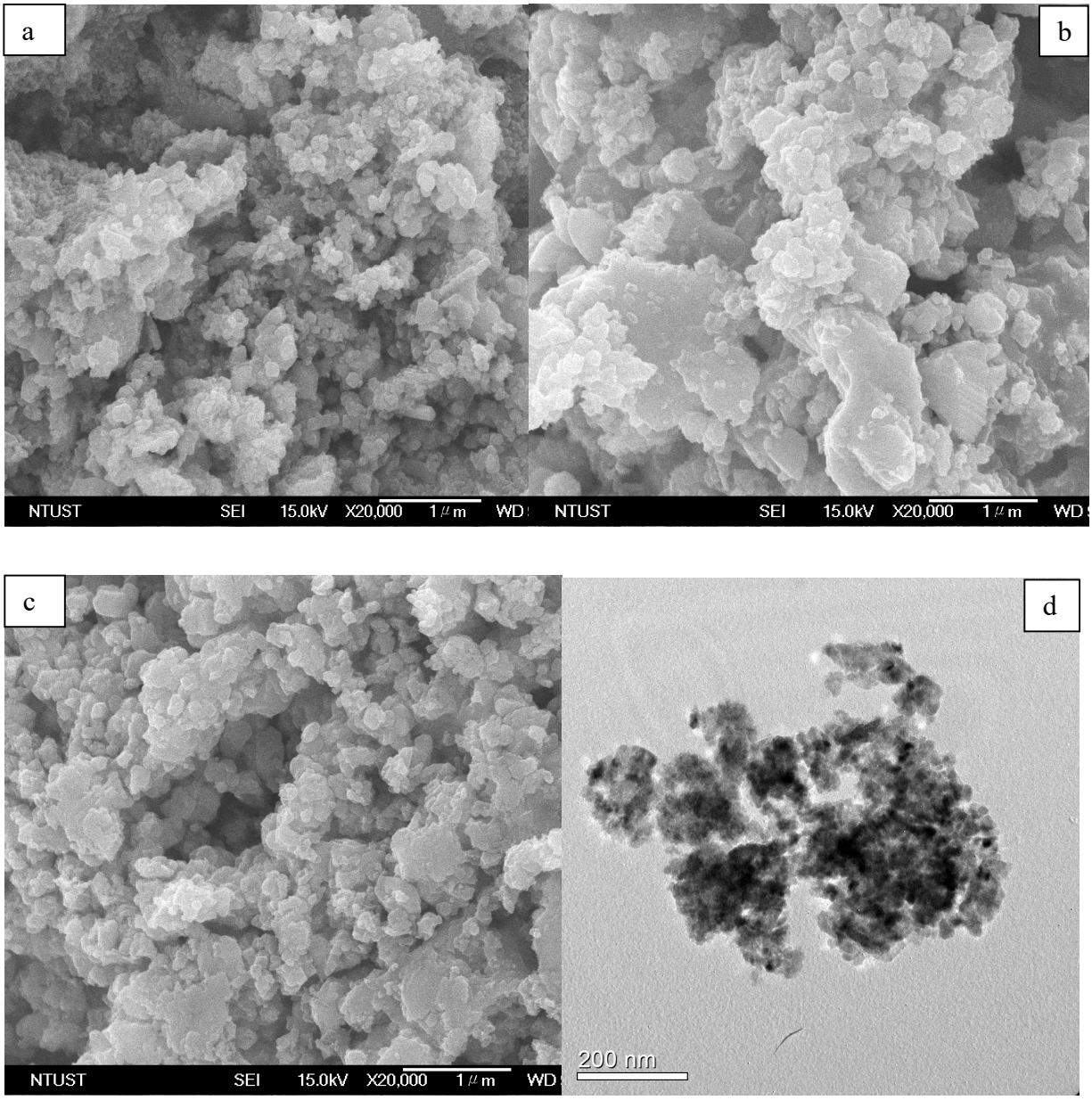

Figure 10. SEM images (a) 1:10, (b) 3:10, (c) 1:2 and (d) TEM image of 1:10 ratios of the synthesized copper oxide nanoparticles.

4.2.4. Energy-dispersive X-Ray Spectroscopy

The chemical composition of biosynthesized CuO Nps was analyzed using EDX. As shown in Figure 11; EDX spectrum result revealed that the green synthesized copper oxide nanoparticles with different ratios contain elements of copper and oxygen confirming the formation and purity of CuO NPs. Furthermore the quantitative data confirmed the formation of CuO instead of other copper oxide.

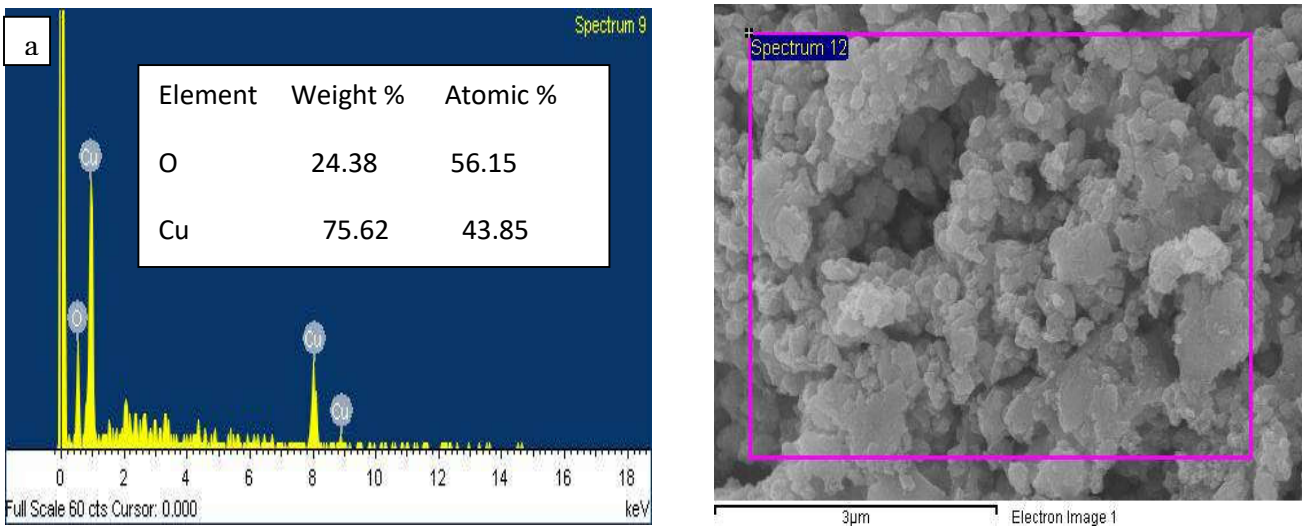

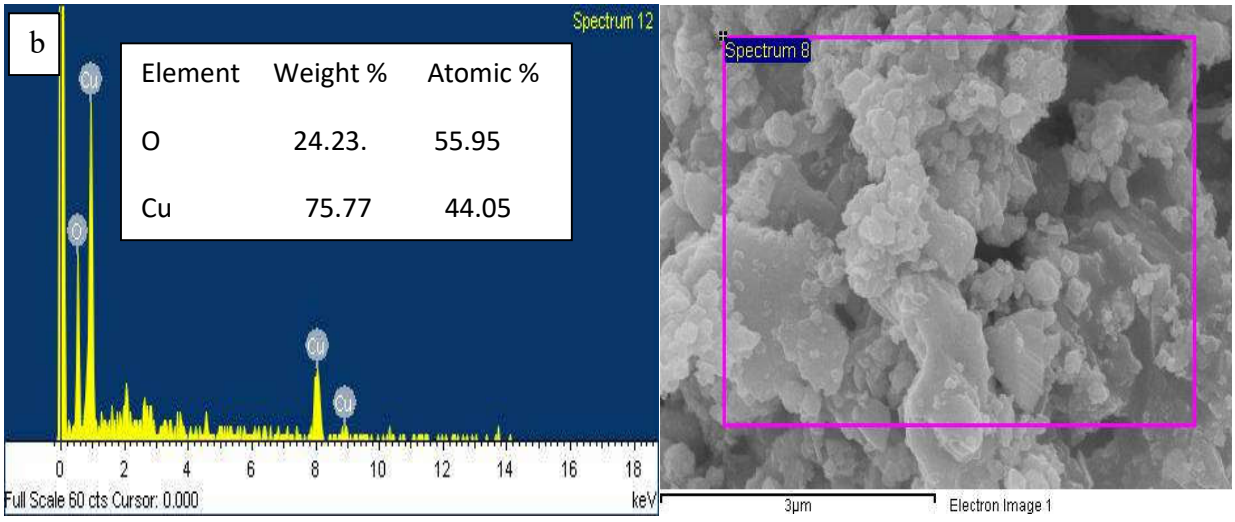

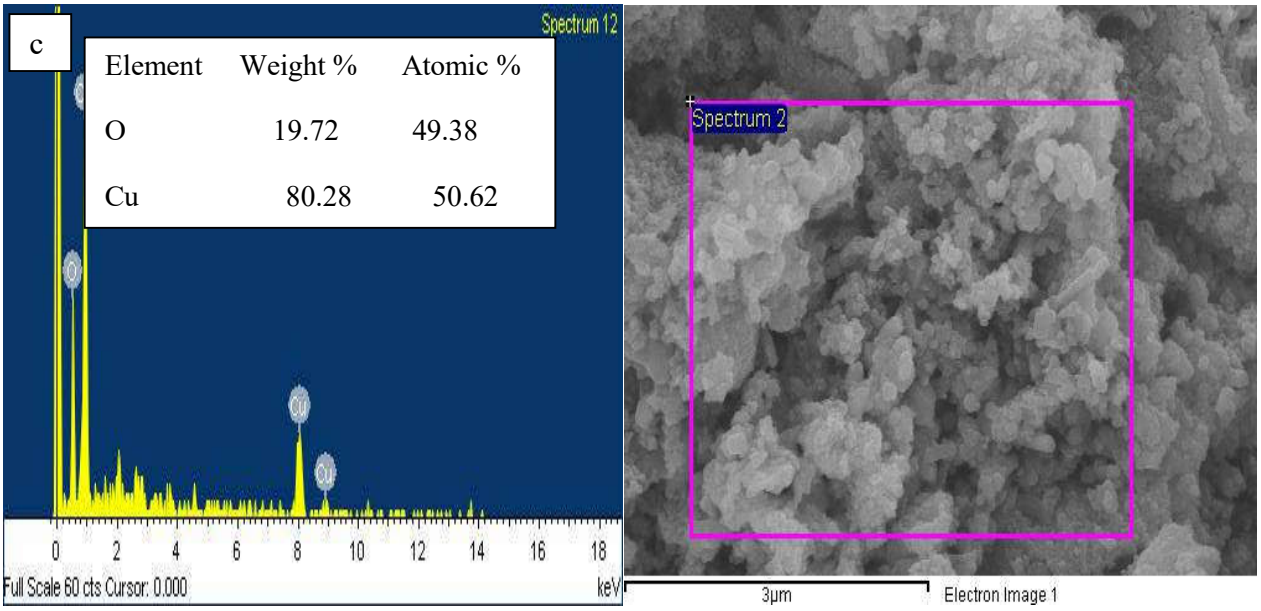

Figure 11. EDX images of (a) 1:10, (b) 3:10 and (d) 1:2 ratios of green synthesized copper oxide nanoparticles.

4.2.5. UV – Visible Spectroscopy Analysis

UV/Vis diffuse absorption edges of the as-synthesized copper oxide nanoparticle were obtained from plot of absorbance against wavelength. The intercept of the tangent line on descending part of the absorption peak at the wavelength axis gives the value of diffuse absorption edge (nm). In such case band gap energy (E_g) of the as-synthesized copper oxide could be obtained from equation 6, (El-Kemary *et al*., 2010).

$$Eg = \frac{\mathbf{1240\ eV}}{\boldsymbol{\lambda_{max}}} \qquad (6)$$

Where, Eg is band gap energy in electron volts and λ_{max} is wavelength (nm) corresponding to absorption edge.

But estimating the band gap using the above approach sometimes may not provide clear tangential line when the peak is not well resolved for the samples. To avoid the difficulties in obtaining band gap energy from UV/Vis absorption spectroscopy in dispersed samples, diffuse reflectance measurements of dry powders can be performed. The optical absorption properties of each of the as-synthesized copper oxide nanoparticle were investigated by using a UV/Vis diffuse reflectance spectrometer in the range of 200-800 nm. Figure 12 a, b and c shows the UV- Vis spectrum of green synthesized CuO NPs with ratio of 1:10, 3:10, and 1: 2, respectively. The nanoparticle showed high absorbance over visible wavelength range which is one of the indications that the NPs are narrowband gap material. Furthermore, it can be observed from the spectra that absorbance increases as the precursor ratio increases that may be due to the dense population of the nanoparticles.

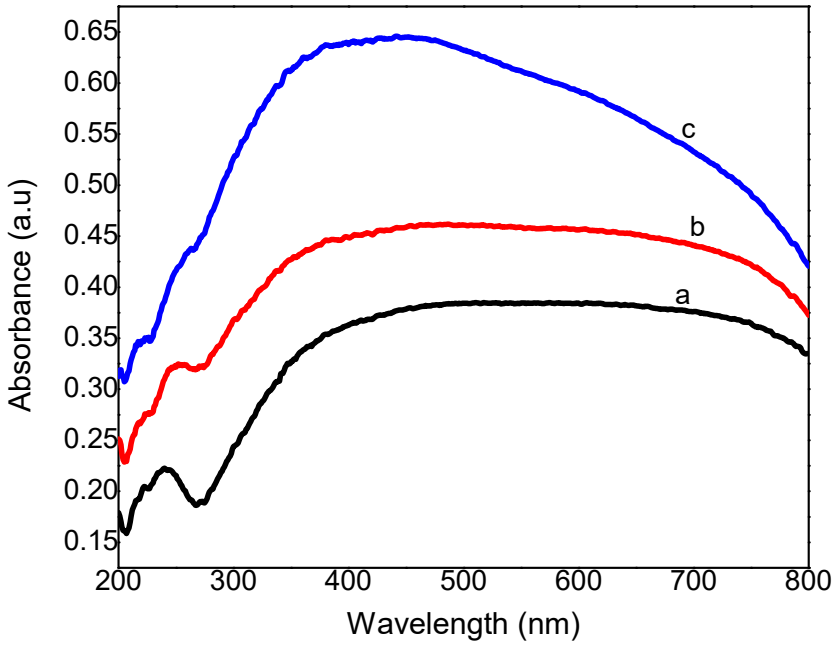

Figure 12. UV-Vis spectra of (a) 1:10, (b) 3:10 and (c) 1:2 ratios of green synthesized CuO nanoparticles

The band gap values of the CuO NPs were determined by analyzing the optical data with the expression for the optical absorbance α and the photon energy hv using Tauc's plot (Zou *et al*., 2015).

$$\alpha h\nu = A\,(h\nu - E_g)^{n/2} \qquad (7)$$

where α is the absorption coefficient, which is proportional to the absorbance, h is the Planck's constant (J.s), *v* is the light frequency (s^{-1}), A is absorbance, E_g the band gap energy and n is a constant related to the electronic inter band transition. n = 2 for an indirect allowed transition (plotted as $(\alpha h\nu)^{1/2}$ versus E_g), n = 3 for an indirect forbidden transition (plotted as $(\alpha h\nu)^{1/3}$ versus Eg), n = 1/2 for a direct allowed transition (plotted as $(\alpha h\nu)^2$ versus E_g), n = 3/2 for a direct forbidden transition (plotted as $(ah\nu)^{2/3}$ versus E_g) (Lopez and Gomez, 2012).

The band gaps of the CuO NPs was then determined by extrapolating the straight line portion of the $(\alpha h\nu)^2$ versus (h*v*) graphs to the (h*v*) axis until $(ah\nu)^{1/n} = 0$, the linear section of this spectrum as shown in the Figure 13 a, b and c respectively.

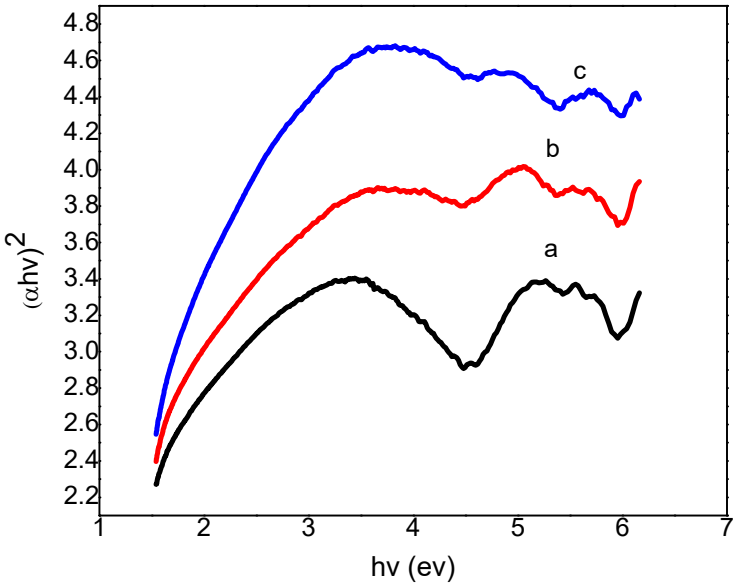

Figure 13. Tauc plots (a) 1:10, (b) 3:10 and (c) 1:2 ratios of green synthesized CuOnanoparticles

Based on Tauc's plot as equation (7) the band gaps of synthesized CuO NPs with ratios 1:10, 3:10 and 1:2 were obtained with 1.31, 1.39 and 1.45 eV respectively by extrapolation. The estimated band gap energy of the synthesized CuO NPs was lower than that was reported in the literature reported. This may comes due to dense population of the nanoparticles but it was between the interval that was reported. These findings are similar with previous reports made on these nanoparticles (Faheem *et al*., 2017). This low band gap of CuO NPs made them to be used as counter electrode (cathode), for collection of electrons, in the fabrication of solar cells.

4.2.6. Fourier Transform Infrared Spectroscopy

FT-IR measurement was performed to identify the possible functional groups that were responsible for reducing and capping of synthesized CuO NPs. Furthermore, FTIR spectra can also be used to identify the characteristics peak of Cu-O bonding as one confirmation technique for the formation of CuO NPs.

Figure 14 a and b shows the FTIR spectra of uncalcinated and calcinated CuO NPs. Based on the FTIR spectrum of CuO NPs, the most significant absorption peak at 531 and 603 cm^{-1}. The phonon bands at correspond to the stretching vibration of Cu–O bond in monoclinic CuO. There is a study reported that CuO (M-O) stretching occurs at 528 cm^{-1} (Sundaramurthy and Parthiban, 2015). The strong peak at (1030 and 1053 cm^{-1}) is due to C-O stretching vibration in carboxylic group and flavanones. The characterized peak observed at (1383 cm^{-1}) is C-N stretching vibration in amine group (Sadeghi *et al*., 2015).The strong band at (1604 and 1638 cm^{-1}) was due to aromatic C=C bending vibration and absorption peaks at 2875 cm^{-1} and 2884 cm^{-1} were attributed to asymmetric and symmetric C-H stretching mode which caused by the phenolic compounds (Sankar *et al*., 2013). The broad band at 3439 cm^{-1} was due to OH stretching vibration in alcohols. This disappeared peak indicates the phytochemical present in the leaf extract, which is involved in reduction and capping of copper oxide nanoparticles.

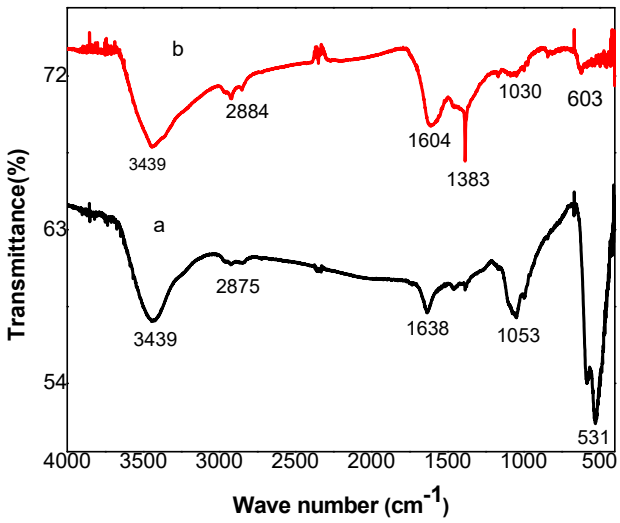

Figure 14. FTIR spectrum of (a) calcinated and (b) uncalcinated 1:10 ratios of synthesized CuO NPs.

4.3. Dye-Sensitized Solar Cells using CuO NPs as Counter Electrode

4.3.1. UV-Vis absorption of Photosensitizers

Natural dye extracts of *kniphofia schemperi* and synthetic dye extracts of crystal violet using ethanol and distilled water, respectively, were used as photo sensitizers in the fabrication of dye-sensitized solar cells in this work. One of the essential requirements of best performing sensitizer is broad and intense absorption in the visible and near-IR region of the solar spectrum (Cremurs, 1977).Figure 15 a and b shows the UV-Vis absorption spectra of the dyes. As observed from UV-Vis spectra, dyes extracted from *kniphofia schemperi* absorb photons in the visible portion of electromagnetic radiation. Similarly, the UV-Vis absorption of crystal violet dye in distilled water solution is shown in Figure 15 b which exhibits strong absorption at 440 nm.

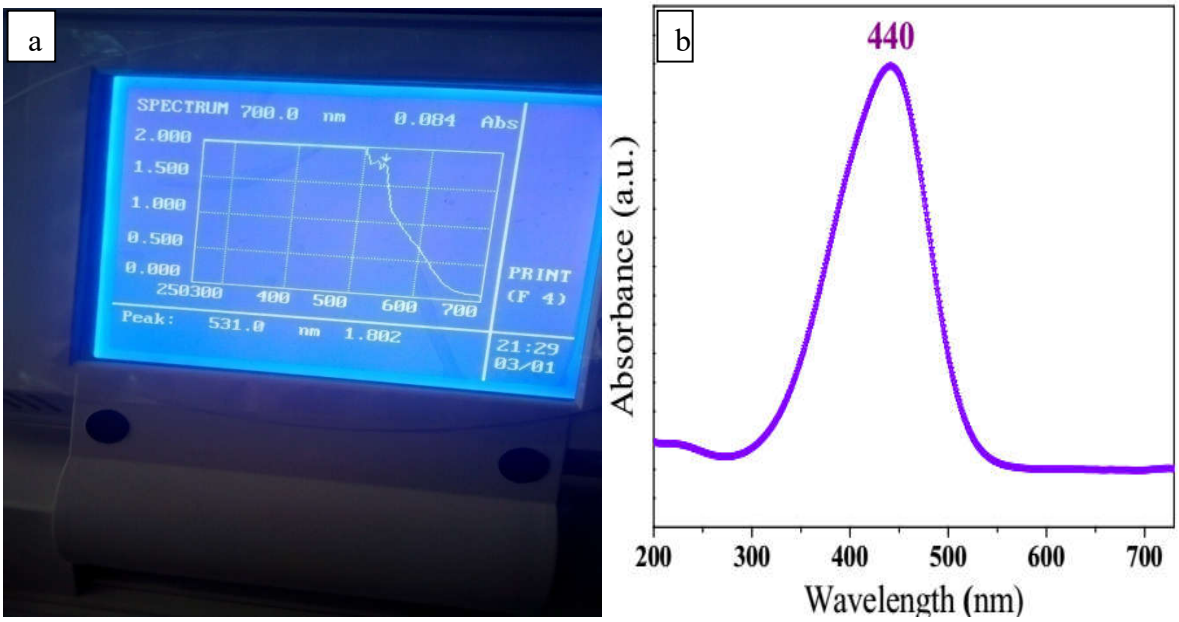

Figure 15.UV-Vis absorption spectra of (a) *kniphofia schemperi* and *(b)* crystal violet dye.

4. 3.2. Current Density -Voltage Characteristics of CuO NPs Based Dye-Sensitized Solar Cells

The photovoltaic tests of the fabricated DSSCs using the natural sensitizers extracted from *kniphofia schemperi* and Crystal violet dye were performed by measuring the current density-voltage (J-V) characteristic curves. The performances of the DSSCs were evaluated by using their short circuit current density (Jsc), open circuit voltage (Voc), and maximum power point from the *J-V* curves and calculated fill factor. The typical current density–voltage (J-V) curves of fabricated DSSCs using natural dyes extracted from *kniphofia schemperi* and Crystal violet dye for each ratio of the as synthesized CuO NPs paste as a counter electrode were tested and their J-V curves are shown below. Figure 16 and 17 a, b and c shows the J-V curve of DSSCs fabricated using CuO NPs as counter electrode which was synthesized in the ratio of (a) 1:10, (b) 3:10 and (c) 1:2 of precursor mass to volume of *catha edulis* extract using crystal violet dye and *kniphofia schemperi* extracted dye photosensitizers respectively.

The photovoltaic parameters, short circuit current (Jsc) and open circuit voltage (Voc), were determined from the J-V curve and fill factor (FF) and power conversion efficiency (η) were calculated from the corresponding parameters. The average short circuit current for the cells is higher in the DSSC where small band gap energy copper oxide based counter electrodes in 1:10 ratio of synthesized CuO NPs was used. The higher Jsc in small band gap energy copper oxide based counter electrode solar cell is due to good energy levels alignment that facilitates charge dissociation (Guo *et al*., 2015). In this ratio the

synthesized CuO NPs resulted in maximum conversion efficiency in both *kniphofia schemperi* and crystal violet photosensitizers.

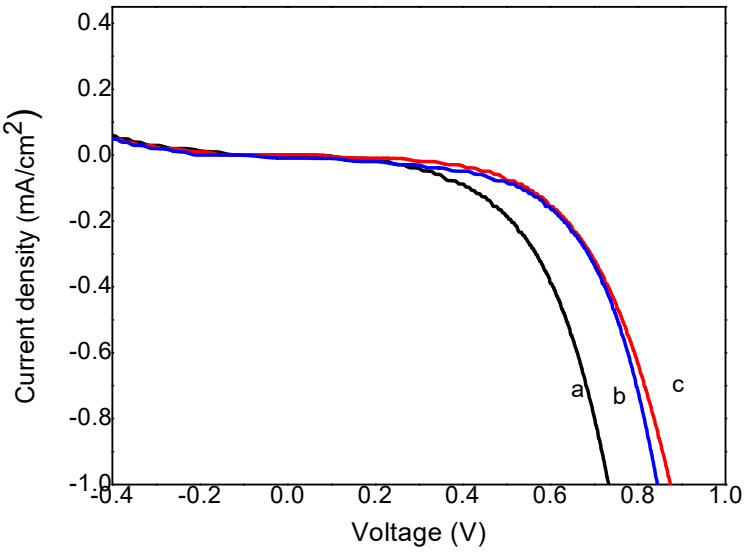

Figure 16. J–V curve of DSSC fabricated with counter electrode based on (a) 1:10, (b) 3:10 and (c) 1:2 ratios synthesized CuO NPs using crystal violet dye.

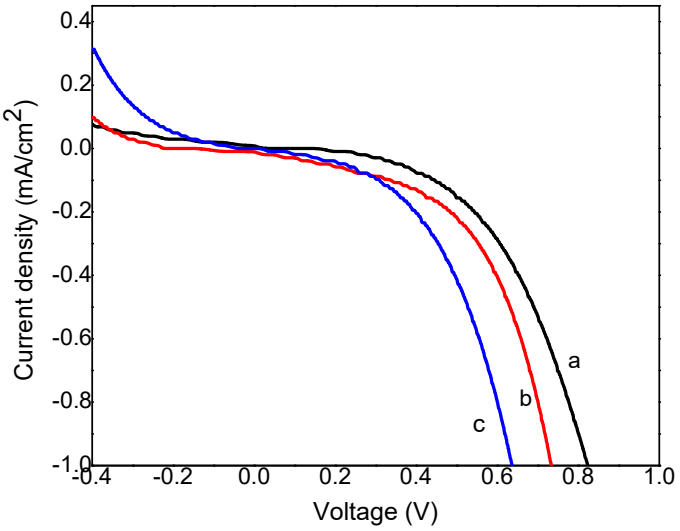

Figure 17. J–V curve of DSSC fabricated with counter electrode based on (a) 1:10, (b) 3:10 and (c) 1:2 ratios synthesized CuO NPs using *Kniphofia schemperi* dye.

Table 4 shows the summary of photovoltaic parameters of DSSCs fabricated using CuO NPs as counter electrode which was synthesized using different ratios of precursor mass to volume of *khat edulis*

Table 4. Photovoltaic parameters of the DSSCs fabricated using CuO NPs as counter electrode and sensitized with natural dyes extracted from *kniphofia schemperi* root and commercial crystal violet dye.

Dyes Used	Solvent	Ratios	J_{sc} (mA/cm^2)	V_{oc}(mV)	P_{max}(mW/cm^2)	FF (%)	η (%)
Crystal Violet Dye	Distilled Water	1:10	3.03×10^{-3}	68	1.2×10^{-1}	58.2	0.12
		3:10	1.29×10^{-3}	46	3.05×10^{-2}	51.4	0.031
		1:2	1.52×10^{-4}	34	2.38×10^{-3}	46.1	0.0024
Kniphofia Schemperi Dye	Ethanol	1:10	2.03×10^{-3}	139	1.65×10^{-1}	67	0.165
		3:10	1.09×10^{-3}	154	7.25×10^{-2}	43.2	0.0725
		1:2	4.04×10^{-4}	110	2.47×10^{-2}	55.6	0.0247

As it can be observed from Table 4, the current density generated from the fabricated DSSCs using CuO NPs as counter electrode is low. The low current generation of the devices could be due to inefficient light harvesting efficiency (LHE) by the dye, inefficient charge injection into TiO_2, or inefficient collection of injected electrons. Furthermore, low LHE can be due to a low dye absorption coefficient over the solar spectrum, a low dye concentration, a thin TiO_2 film to support large concentration of adsorbed dye which absorbs a significant fraction of the incident light, insufficient light scattering within the film, absorption of light by TiO_2 or the redox electrolyte, and dye degradation (Halme *et al*., 2010).

4.3.3. Incidence Photon to Current Conversion Efficiency (IPCE)

The incident photon to current conversion efficiency (IPCE) of natural and synthetic pigments sensitized DSSCs with TiO_2 photoelectrode and CuO nanoparticles based counter electrode was calculated using Equation (4) from experimentally generated data. Figure 18 and 19 show the action spectra for the DSSCs sensitized using *Kniphofia schemperi* and crystal violet dyes respectively.

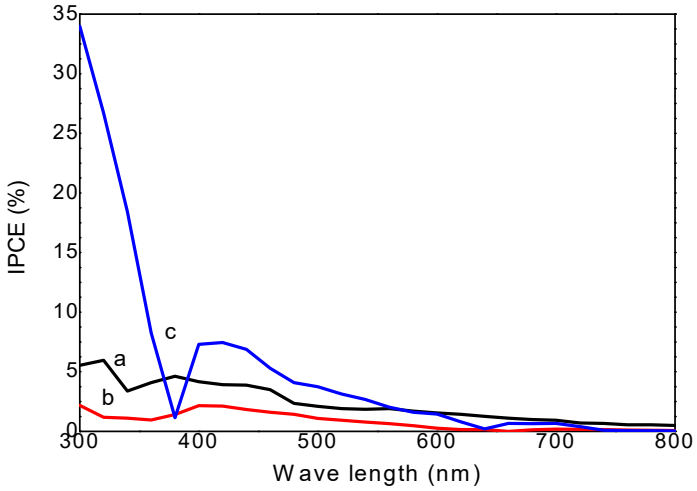

Figure 18. IPCE of CuO (a) 1:10, (b) 3:10 and (c) 1:2 ratios based DSSCs sensitized by crystal violet dye with water

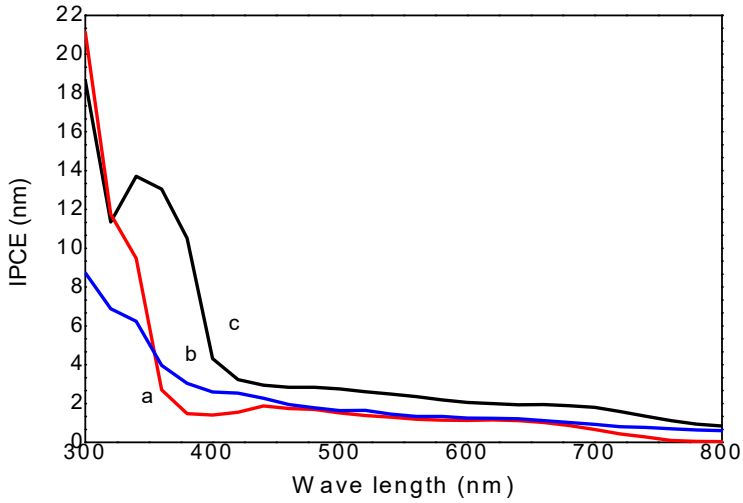

Figure 19. IPCE of CuO (a) 1:10, (b) 3:10 and (c) 1:2 ratios based DSSCs sensitized by *Kniphofia schemperi* dye with ethanol

As observed from Figure 18 and 19, IPCE of the fabricated DSSCs are very low that of course agrees with the low current density of the devices.

5. CONCLUSION

Green synthesis was successfully employed to synthesize CuO NPs by the leaves extract of *catha edulis* plant in aqueous medium and synthesized CuO NPs utilized was used as electrocatalytic materials for the preparation of counter electrode in DSSC. The synthesized CuO NPs were extensively characterized in terms of morphology, crystalline nature, structural, and photovoltaic properties using various experimental tools. The synthesized CuO NPs possess well crystalline nature which is perfectly matched to spherical structure of bulk CuO. Moderately medium solar to electrical energy conversion efficiency of 0.165% with short circuit current density (J_{SC}) of 2.03 x 10^{-3} mA/cm^2, open circuit voltage (V_{OC}) of 139 mV and fill factor (FF) of 67% was recorded in the DSSC fabricated with synthesized CuO NPs based counter electrode. Therefore, this work showed that *Catha edulis* can be used for bio-synthesis of CuO NPs which is low cost & ecofriendly method of nanoparticle synthesis. Furthermore, this work showed that the biosynthesized CuO NPs using *Catha edulis* were applied as efficient counter electrode for the fabrication of DSSCs that may replace other expensive counter electrodes like platinum which are used for the fabrication of DSSCs.

REFERENCE

Akinori K., Kumara G. R. and Tennakone K., (2005).The use of fossil fuels in the world. *Japanese Institute of Fundamental Study,* 3: pp. 425-432.

Amkamwar B., Damle C., Ahmad A. and Sastry M., (2005). Biosynthesis of gold and silver nanoparticles using Emblicaofficinalis fruit extract, their phase transfer and transmetallation in an organic solution. *Journal of Nanoscience and Nanotechnology*, 5: pp. 1665-1671.

Ansilin S., Nair J. K., Aswathy C., Rama V., Peter J., Persis J., (2017). Green Synthesis and Characterisation of Copper Oxide Nanoparticles using *Azadirachta indica* (Neem) Leaf Aqueous Extract. *Journal of Nanoscience and Technology*, 2: pp. 221-223.

Aparna Y., Enkateswara Rao, K.V. and Srinivasa Subbarao P., (2016).Synthesis and characterization of CuO nanoparticles by novel sol gel method. *Journal of Environmental Science and Biotechnology,* 48: pp. 30-33.

Ardo S. and Meyer G. J., (2009). Photodriven heterogeneous charge transfer with transitionmetal compounds anchored to TiO_2 semiconductor surfaces. *Chemical Society Review,* 38: pp. 115-164.

Baker N., (1996). Photosynthesis and the Environment, *Kluwer Academic Publisher*, Netherland, pp. 1-491.

Baker S., Rakshith D., Kavitha K. S., Santosh P., Kavitha H. U., Rao Y. and Satish S., (2013). Plants emerging as nanoparticles towards facile route in synthesis of nanoparticles. *BioImpacts*, 3: pp 111-115.

Berhanu M., Aregash E., Alyi M., (2014). Socio-Economic Impact of Khat in Mana District, Jimma Zone, South Western Ethiopia. *Discourse Journal of Agriculture and Food Sciences*, 2: pp. 21-32.

Borgohain K., Murase N., Mahamuni S., (2002). Synthesis and properties of Cu_2O quantum particles. *Journal of Applied Physics*, 92: pp. 1292 -1297.

Burda C., Chen X., Narayanan R. and El-Sayed M.A., (2005).Chemistry and properties of nanocrystals of different shapes. *Chemistry Review,* 105: pp. 1025–1102.

Chappel S., Ofir A. and Zaban, (2005). Extending the current Collector into the Nanoporous Matrix of Dye Sensitized Electrodes, *Journal of Physics Chemistry*, 109: pp. 1643-1647.

Cho S., (2013). "Optical and electrical properties of CuO thin films deposited at several growth temperatures by reactive RF magnetron sputtering." *Metals and Materials International*, 19: pp 1327–133.

Cremers D. A., (1977).Defense technical information center.

Devi H. S. and Singh T. D., (2014). Synthesis of copper oxide nanoparticles by a novel method and its application in the degradation of methyl orange. *Advanced Electronic and Electrical Engineering*, 4: pp. 1- 83.

El- Kemary M., H. El-shamy and I. El-mahasseb (2010).Photocatalytic degradation of Ciprofloxacin drug in water using ZnO nanoparticles. *Journal of Luminescence*, 130: pp. 2327- 2331.

Elhassan M. M., Abdelwahab S.I., Al-sanousi R., (2014). In vitro hepatotoxcity of Catha edulis Forsk. (Khat) phenolic-rich extract on human hepatocytes. *Journal of Applied Pharmaceutical Science*, 4: pp. 42-46.

Enerdata, Global Energy Intelligence, World Energy Use in 2010: Over 5% Growth May, 2011.

Faheem I., Sammia S., Shakeel A. K., Waqar A., Sabah Z., (2017). Green synthesis of copper oxide nanoparticles using Abutilon indicum leaf extract: Antimicrobial, antioxidant and photocatalytic dye degradation activities. *Tropical Journal of Pharmaceutical Research,* 16: pp. 743-753.

Fayaz M A., Girilal M., Rahman M., Venkatesanc R. and Kalaichelvan P.T., (2011). Biosynthesis of silver and gold nanoparticles using *thermophilicbacterium Geobacillus stearothermophilus*. *Process Biochemistry,* 46: pp. 1958–1962..

Ghorbani H. R., (2014). Chemical synthesis of Copper nanoparticles. *Orientation in Journal of Chemistry*, 30: pp. 755- 803.

Gong J., Liang J., Sumathy K., (2012). Review on dye sensitized solar cells (DSSCs) fundamental concepts and novel materials, Renew and Sustain Energy Review. *Inorganic Chemistry*, 16: pp. 5845-5848.

Gratzel M., (2005). Solar energy conversion by dye-sensitized photovoltaic cells. *Inorganic Chemistry,* 44: pp. 6841-6851.

Guo S. Q., Sun M.Q., Gao G. D., Liu L., (2015). Scalable low-cost CdS nanospheres@ grapheme nanocomposites counter electrode for high efficiency dye-sensitized solar cells. *Electrochimica Acta,* 176: pp. 1165- 1170.

Halme J., Vahermaa P., Miettunen K. and Lund P., (2010). Natural dye sensitized phothoelectrochemical cells based on zinc oxide nanoparticles. *Advanced Materials*, 22: pp. 210-221.

Hee J. K., Karthick K.V., Hemalatha C., Justin R., Venkatesan S. P., (2013). Natural Dye Extracted from Rhododendron Species Flowers as a Photosensitizer in Dye Sensitized Solar Cell. *International Journal of Electrochemical Society,* 8: pp. 6734-6743.

Hodes G., (2007). When small is different: Some recent advances in concept and applications of nanoscale phenomena. *Advanced Material*, 19: pp. 639-655.

Hsiao M.T., Chen S.F., Shieh D.B. and Yeh C.S., (2006). One-pot synthesis of hollow Au_3Cu1 spherical-like and biominerabotallackite $Cu_2(OH)_3Cl$ flowerlike architecture exhibiting antimicrobial activity. *Journal of physical Chemistry, 110*: pp. 205-210.

Hu J. P., Payne D. J., Egdell R. G., (2008). On-site interband excitations in resonant inelastic X-ray scattering from CuO. *Physical Review*, 77: pp 115 - 155.

Hutchison J. E., (2008). Greener nanoscience: a proactive approach to advancing applications and reducing implications of nanotechnology. *ACS Nano*, 2: pp. 395-402.

Ibrahim H. M. M., (2015). Green synthesis and characterization of silver nanoparticles using banana peel extract and their antimicrobial activity against representative microorganisms. *Journal of Radiation Research and Applied Sciences*, 8: pp. 265-275.

Ismat Z., Lutfun N., Sarwaruddin C., Gafur M., Nuruzzaman K., Ruhul A., (2015). Preparation and characterization of copper oxide nanoparticles synthesized via chemical precipitation method. *Open Access Library Journal,* 2: pp. 2-8.

Ito T., Yamaguchi H., Okabe K., Masumi T., (2008). Single-crystal growth and characterization of Cu_2O and CuO. *Journal of Materials Science*, 33: pp 3555–3566.

Jayalakshmi and Yogamoorthi A., (2014).Green synthesis of copper oxide nanoparticles using aqueous extract of flowers of *Cassia alata* and particles characterization. *Int*ernational *J*ournal *of Nanomaterials and Biostructure*, 4: pp. 66-80.

Jitendra K. S., Shaheer M. A., Ameen S., Pratibha S. and Gurdip S., (2015). Green synthesis of CuO nanoparticles with leaf extract of Calotropis gigantea and its dye-sensitized solar cells applications.*Journal of Alloys and Compounds*, 632: pp. 321-325.

Joshua P., Krishnan J., Vidhya S., Uthrakumar D. J., (2014). Novel synthesis of tenorite (CuO) nanoparticles by wet chemical method. *International Journal of Chemical Technology Research*, 6: pp. 2002-2011.

Jyoti M., Vijay D., Radha S., (2014). Synthesis of copper oxide nanoparticles using simple chemical route. *International Journal of Scientific & Engineering Research*, 5: pp. 928-930.

Katwal R., Kaur H., Sharma G., Naushad M. and Pathania D., (2015). Electrochemical synthesis copper oxide nanoparticles for enhanced photocatalytic and antimicrobial activity. *Journal of Industrial and Engineering Chemistry,* 31: pp. 173-184.

Kessler R., (2011). Engineered Nanoparticles in Consumer Products: Understanding a New Ingredient. *Environmental Health Perspectives,* 119: pp. 120-125.

Khodashenas B. and Ghorbani H. R., (2014). Synthesis of copper nanoparticles: an overview of the various methods. *Korean Journal of Chemical Engineering*, 31: pp. 1105–1109.

Koffyberg F. P. and Benko F. A., (2013). A photoelectrochemical determination of the position of the conduction and valence band edges of p-type CuO. *Journal of Applied Physics*, 53: pp. 1168-1173.

Kotov Y. A., (2003). Electric explosion of wires as a method for preparation of nanopowders. *Journal of Nanoparticle Research*, 5: pp. 539–550.

Li J.L., Liu L., Yu Y., Tang Y.W., Li H.L., Du F.P., (2005). Preparation of highly photocatalytic active nano-sized TiO2-Cu2O particle composites with a novel electrochemical method. *Electrochemical Community*, 6: pp. 940-942.

Longo C. and De Paoli M. A., (2003). Dye-Sensitized Solar Cells: a Successful Combination of Materials. *Journal of Brazil Chemistry Society*, 14: pp. 889-901.

Lopez R. and Gomez R., (2012). Band-gap energy estimation from diffuse reflectance measurements on sol-gel and commercial TiO_2: a comparative study. *Journal of Sol-Gel Science and Technology*, 61: 1-7.

Ludin N. A., (2014). Review on the development of natural dye photosensitizer for dye-sensitized solar cells. *Renewable and Sustainable Energy Reviews*, 31: pp. 386-396.

Macht B., Turrion M., Barkschat A., Salvador P., Ellmer K. and Tributsch H., (2002). Effects of water intrusion on the charge-carrier dynamics, performance, and stability of dye sensitized solar cells. *Solar Energy Materials and Solar cells,* 73: pp. 163-173.

Mahmoud N., S. Mohammad S., Akbar R. V., (2015). Green synthesis of CuO nanoparticles by aqueous extract of *Anthemisnobilis* flowers and their catalytic activity for the A^3 coupling reaction. *Journal of Colloid and Interface Science,* 459: pp. 183-188.

Makarov V. V., Love A. J., Sinitsyna O. V., Makarova S. S., Yaminsky I. V., (2014). Green nanotechnologies: synthesis of metal nanoparticles using plants. *ActaNature*, 6: pp. 35-41.

Mary N. and Rosana, (2015). Pigments for Generating Electric Power - An Overview. *Research Journal Pharmacology Biology and Chemistry Society,* 6: pp. 691-698.

Meidan Y., Xiaoru W., Mengye K. Wang J., (2015). Recent advances in dye-sensitized solar cells: from photoanodes, sensitizers and electrolytes to counter electrodes. *Materials Today*, 18: pp. 155-162.

Mishina E. D., Nagi K., Nakabayashi S., (2011). Self-Assembled Cu/Cu_2O Multilayer's: Deposition, Structure and Optical Properties. *NanoLetter*, 1: pp. 401-404.

Mohanpuria P., Rana K.N. and Yadav S.K., (2008). Biosynthesis of nanoparticles: technological concepts and future applications. *Journal of Nanoparticle Research,* 10: pp. 507- 517.

Muniz M., Miranda ·C., Gellini A., Simonelli M., Tiberi F., Giammanco E., (2014). Characterization of copper nanoparticles obtained by laser ablation in liquids. Journal of Applied Physics, 110: pp. 829-833.

Murakami T. N. and Grätzel M., (2008). Counter electrodes for DSSC application of functional materials as catalysts. *Inorganic Chemical Acta*,361: pp. 569-572.

Naika H. R., Lingaraju K., Manjunath K., Kumar D., Nagaraju G., Suresh D. and Nagabhushana H., (2015). Green synthesis of CuO nanoparticles using *Gloriosa superba* L. extract and their antibacterial activity. *Journal* of *Taibah*an *University of Science,* 9: pp 7-15.

Onah D.U. and Ugwu E.I., (2015). Optical characteristics of CuO thin film prepared by Chemical spray pyrolysis. *Journal of nanomaterials*, 3: pp. 59- 62.

Parashar V., Prashar R., Sharma B. and Pandey A.C., (2009). Parthenium leaf extract mediated synthesis of silver nanoparticles: a novel approach towards weed utilization. *Digest journal of nanomaterials and biostructures*, 4: pp. 45-50.

Park N.G., van de Lagemaat J. and Frank A. J., (2000). Comparison of dye-sensitized rutile and anatase based TiO_2 solar cells. *Journal of Physical Chemistry*, 104: pp. 8989-8994.

Preview of World Energy Outlook 2018.

Rahman A., Ismail A. and Jumbianti D., (2009).Synthesis of copper oxide nanoparticles by using *Phoridium cyanibacterium*. *Journal of Chemistry*, 9: pp. 315- 355.

Rao A. N. S. and Venkatarangaiah V. T., (2014).The effect of ceyltrimethylammonium bromide on size and morphology of ZnO and CuO. *Journal of Electrochemical Science and Engineering*, 4: pp. 97-110.

Rao G.N., Yao Y., Chen J., **(**2009).Evolution of size, morphology, and magnetic properties of CuO nanoparticles by thermal annealing. J*ournal of Applied Physics, 105*: pp. 901-903.

Realpe A., Salamanca A., Acevedo M., (2015). Effect of electrolyte type on the hydrogen production using a plate electrolyzer. *International Journal of Applied Engineering*, 10: pp. 871-880.

Rosi NL. and Mirkin C. A., (2005). Nanostructures in biodiagnostics. *Chemical Review*. 105: pp. 1547–1562.

Ruiz P., Katsumiti A., Nieto J. A. and Bori J., (2015). Short-term effects on antioxidant enzymes and long-term genotoxic and carcinogenic potential of CuO nanoparticles compared to bulk CuO. *Material Environmental Research,* 111: pp. 107- 120.

Sadeghi B., Rostami A., Momeni S.S., (2015). Facile green synthesis of silver nanoparticles using seed aqueous extract of Pistacia atlantica and its antibacterial activity. *Spectrochim Acta*, 134: pp. 326-332.

Sangiliyandi G., Kalishwaralala K., Vaidyanathana R., (2009). Biosynthesis, purification and characterization of silver nanoparticles using *Escherichiacoli*. *Colloids and Surfaces Biointerfaces*, 74: pp. 328–335.

Sankar R., Karthik A., Prabu A., Karthik S., Shivashangari K.S., Ravikumar V., (2013). Origanum vulgare mediated biosynthesis of silver nanoparticles for its antibacterial and anticancer activity. *Colloids Surface*, 108: pp. 80- 84.

Sankar R., Manikandan P., Malarvizhi V., Fathima T., Shivashangari K. S., Ravikumar V., (2014). Green synthesis of colloidal copper oxide nanoparticles using Carica papaya and its application in photocatalytic dye degradation. *Spectrochim Acta Mol Biomol Spectrosc*, 121: pp. 746-750.

Sen J., Prakash P. and De N., (2015). Nano clay composite and phytonanotechnology: a new horizon to food security issue in Indian agriculture. *J*ournal of *Globa*l *Bioscience*, 2: pp. 187-190.

Shankar S., Rai A., Ahmad A., Sastry M., (2004). Rapid synthesis of Au, Ag, and bimetallic Au core-Ag shell nanoparticles using Neem (*Azadirachtaindica*) leaf broth. *Journal of Colloid Interface Science*, 275: pp. 496-502.

Song X., Sun S., Zhang W., (2004). Synthesis of Cu $(OH)_2$ nanowires at aqueous-organic interfaces. *Journal of Physical Chemistry*, 108: pp. 5200–5205.

Subhan A., Ahmed T., Awal R., Nizam U., (2014). Synthesis, structure, luminescence and photophysical properties of nano CuO·ZnO· $ZnAl_2O_4$ multi metal oxide. *Journal of Luminescence*, 146: pp. 123-127,

Sundaramurthy N. and Parthiban C., (2015). Biosynthesis of copper oxide nanoparticles using *Pryus Pyrifolia* leaf extract and evolve the catalytic activity. *International Research Journal of Engineering and Technology,* 2: pp. 332-338.

Survey of Energy Resources, World Energy Council 2016.

Taleb C., Pettai M. and Pileni P., (1998).Nanoparticles and nanostructured films preparation. *Characterization applied Chemistry,* 22: pp. 1203-1203.

Tang X.L., Ren L., Sun L.N., (2006). A solvothermal route to Cu_2O nanocubes and Cu nanoparticles. *Chemical Research in Chinese Universities*, 22: pp. 547- 551.

Tennakone K., Kumara G. R.R., Kottegoda A., (2009). An efficient dye-sensitized photoelectrochemical solar cell made from oxides of tin and zinc. *Chemical Community*, 15: pp. 15–16.

Thi H., and Viet T., (2014). Copper oxiden prepared by solution methods, some properties, and potential applications: a brief review. *International Scholarly Research Notices,* 93: pp. 172-177.

Uskokovic V., (2008). Nanomaterials and Nanotechnologies: Approaching the crest of this big wave. *Current Nanoscience*, 4: pp. 119-129.

Vahermaa J. P., Miettunen K., Lund P., (2010). Interface electric properties of Si/organic hybrid solar cells using impedance spectroscopy analysis. *Advanced Materials*, 22: pp. 210-221.

Valodkar M. R., Jadeja N. and Thounaojam M. C., (2011). Biocompatible synthesis of peptide capped copper oxide nanoparticles and their biological effect on tumor cells. *Materials Chemistry and Physics*, 128: pp. 83–89.

Vedpriya A., (2010). Living Systems: eco-friendly nanofactories. *Digest Journal of Nanomaterials and Biostructures*, 5: pp. 9–21.

Veerasamy R., Xin T. Z., Gunasagaran S. and Dhanaraj S., (2011).Biosynthesis of silver nanoparticles using mangosteen leaf extract and evaluation of their antimicrobial activities. *Journal of Saudi Chemical Society*, 15: pp. 113–120.

Wasan M., Khilkala Ȧ., Ghaleb A., Al-Dahash Ȧ. and Sahib N., (2014). Preparation and characterization of CuO nanoparticles by laser ablation in NaOH aqueous solution. International *Journal of Current Engineering and Technology*, 4: pp. 2577-2579.

William A., Vallejo L., Cesar A., Quiñones S. and Johann A., (2014).The Chemistry and Physics of Dye-Sensitized Solar Cells.

Willis R. L., (2002). Functional properties of nanocrystalline metal oxide films for dye sensitized solar cells. *Imperfect Collision,* 106: pp. 4353-4356.

Won Y., Rho H., Ho S. K., Woo J., Chung J., Sang S. and Bong H., (2015). ” Recent Progress in Dye Sensitized Solar Cells for Improving Efficiency: TiO2 Nanotube Arrays in Active layer.”*Journal of Nanomaterials*, 2015: pp. 1-17.

Wu J., Li Q., Hao L. S., (2008). High-performance polypyrrole nanoparticles counter electrode for dye-sensitized solar cells. *Journal of Power Sources,* 181: pp. 170- 172.

Yunfang W., Xiuli L., Yawen W. and Caimei F., (2013). Novel visible-light $AgBr/Ag_3PO_4$ hybrids photocatalysts with surface plasma resonance effects. *Journal of Solid State Chemistry*, 202: pp. 51-55.

Zou Z., Qiu Y., Xie C., Xu J., Luo Y., Wang C. and Yan H., (2015). CdS/TiO_2 nanocomposite films and its enhanced photoelectric responses to dry air and formaldehyde induced by visible light at room temperature. *Journal of Alloys Compound*, 645: pp. 17-23.